The isotache approach.
Where are we 50 years after its development by Professor Šuklje?
(2006 Prof. Šuklje's Memorial Lecture)

Serge Leroueil
Université Laval, Ste-Foy, Québec, Qué., G1K 7P4, Canada

ABSTRACT
Fifty years after its development by Professor Šuklje, this Paper examines the applicability of the isotache model to geotechnical engineering. Laboratory tests and well documented case histories for which high quality samples were available tend to confirm the validity and the applicability of the model during both primary and secondary consolidation. Moreover, it appears that the isotache model can be extended to take into account the effect of temperature into an isotache-isotherm model. It also appears that these models apply to the general behaviour of soils.

Keywords: clays, consolidation, settlements, strain rate effects, temperature effects, elasto-visco-plasticity

1 INTRODUCTION

When a clay sample is suddenly loaded one-dimensionally, its decrease in void ratio with time is typically as shown in Fig. 1. During primary consolidation, settlement is controlled by dissipation of excess pore pressures and Darcy's Law. During secondary consolidation, the rate of settlement is controlled by soil viscosity. However, as settlement requires hydraulic gradient, excess pore pressures also exist during that stage. Secondary consolidation is characterised by the slope of the consolidation curve, the secondary compression index $C_{\alpha e} = \Delta e/\Delta \log t$.

Mesri & Godlewski (1977) showed that $C_{\alpha e}$ is related to the compression index of the soil and more precisely that the ratio $C_{\alpha e}/C_c$ is a constant for a given soil. This has been confirmed for a large variety of geomaterials by Mesri and co-workers, and many other researchers. Figure 2 shows an example for two eastern Canada clays. An interesting aspect is that, as indicated in Table 1, $C_{\alpha e}/C_c$ remains within a narrow range for each soil type (Mesri, 1987; Mesri et al., 1995). It is typically equal to 0.04 in inorganic clays, takes larger values in organic soils and lower values in granular soils.

An important question is: "What happens when a thicker soil layer, such as the one under an embankment, is loaded in a similar manner?" As indicated by Ladd et al. (1977) and by Jamiolkowski et al. (1985), there are two extreme possibilities (see Fig. 3). "Hypothesis A assumes that creep occurs only after the end of primary consolidation …" and consequently that the stress-strain curve followed in situ is the same as that obtained in the laboratory on small specimens at the end of primary consolidation. "Hypothesis B assumes that some sort of "structural viscosity" is responsible for creep, that this phenomenon occurs during pore pressure dissipation, and therefore that the strain at the end of primary consolidation increases" with sample thickness. As can be seen on Fig. 3, the magnitudes of settlement at the end-of-primary consolidation calculated according to the two theories may differ significantly.

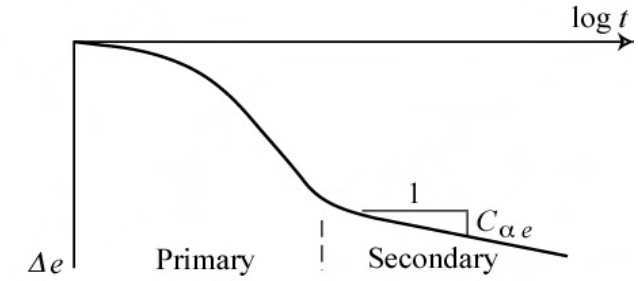

Figure 1. Consolidation curve

Several rheological models have been suggested to describe the compressibility of clays in

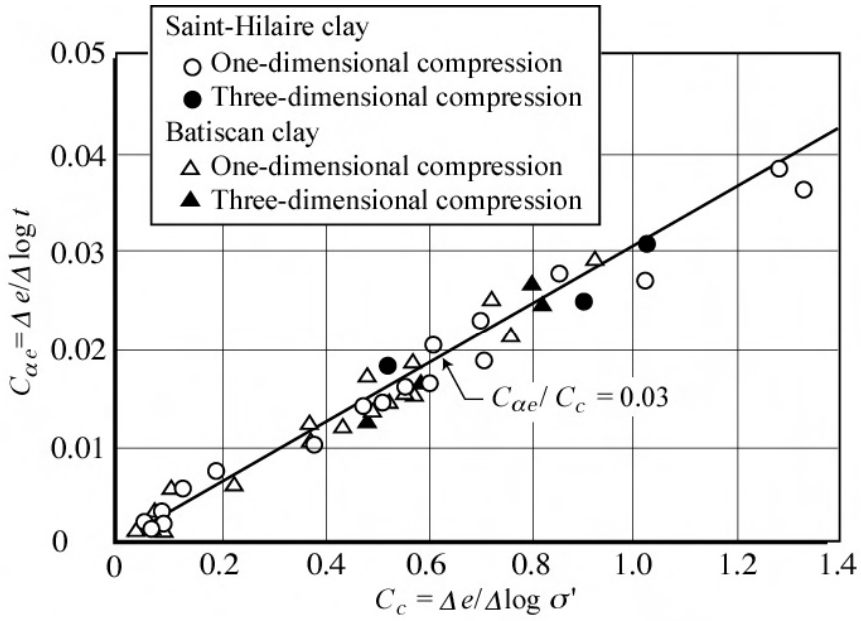

Figure 2. Relationship between secondary compression index $C_{\alpha e}$ and compression index C_c (from Mesri *et al.*, 1995)

Table 1. Viscous parameters for geotechnical materials

Material	$C_{\alpha e}/C_c$ equal to $\alpha = \Delta \log \sigma_p'/\Delta \log \dot{\varepsilon}$	$\frac{\Delta \sigma'}{\sigma'}/\Delta \log \dot{\varepsilon}$ (%)
Granular soils including rockfill	0.02 ± 0.01	2.3 – 7.2
Shale and mudstone	0.03 ± 0.01	4.7 – 9.6
Inorganic clays and silts	0.04 ± 0.01	7.2 – 12.2
Organic clays and silts	0.05 ± 0.01	9.6 – 14.8
Peat and muskeg	0.06 ± 0.01	12.2 – 17.5

Note: types of material and $C_{\alpha e}/C_c$ values are from Mesri *et al.*, 1995.

one-dimensional conditions. Simply, four families can be defined. If e is the void ratio, σ'_v the vertical effective stress, t the time, $\dot{e} = \delta e/\delta t$ and $\dot{\sigma}'_v = \delta\sigma'_v/\delta t$, these families can be represented by the following equations:

$$R(\sigma'_v, e) = 0 \quad (1)$$

$$R(\sigma'_v, e, t) = 0 \quad (2)$$

$$R(\sigma'_v, e, \dot{\sigma}'_v, \dot{e}) = 0 \quad (3)$$

$$R(\sigma'_v, e, \dot{e}) = 0 \quad (4)$$

For natural clays in which the initial void ratio is well defined, these equations can also be expressed in terms of volumetric strain rather than in terms of void ratio. Equation (1) is representative of models in which the effective stress-void ratio response of the soil is unique and independent of time or strain rate. This is the case for the classical Terzaghi theory of consolidation. Koppejan (1948), Bjerrum (1967) and Hansen (1969) have proposed models represented by Equation (2) in which the void ratio is a function of the effective stress and time. A major difficulty may be encountered with these models when applied load varies with time and that an origin for time has to be defined.

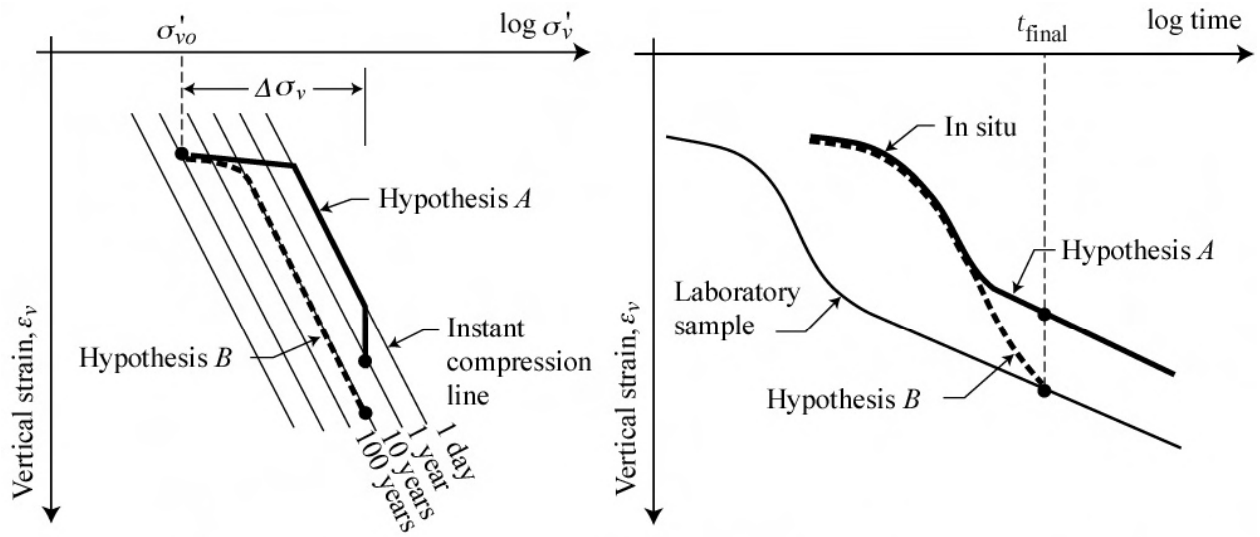

Figure 3. Consolidation of clay layers of different thicknesses according to Hypothese *A* and *B* (after Ladd *et al*., 1977)

The models corresponding to Equations (3) and (4) overcome this difficulty since the behaviour of the material then depends only on its present conditions and is not a function of previous history. Taylor & Merchant (1940) were the first to suggest a model of the type represented by Equation (3) in which the rate of change in void ratio is a function of the effective stress, the void ratio and the rate of change in effective stress. This suggestion has been followed by several researchers, Gibson & Lo (1961) in particular. Models corresponding to Equation (4) show a unique relationship between the effective stress, the void ratio and the rate of change in void ratio; they can be represented in a e-σ'_v diagram by $\dot{e}$ = constant lines called isotaches by Šuklje (1957, 1969a, 1982). Various equations have been suggested to define these isotaches. The first and simplest corresponds to Taylor's theory B (1942):

$$\dot{e} = a\sigma'_v + be + c \qquad (5)$$

More complex equations have been suggested, in particular by Barden (1965), Šuklje (1969b), Battelino (1973) and Hawley & Borin (1973).

Figure 4 (lower part) shows a set of isotaches obtained by Šuklje (1957) for a lacustrine chalk sample. Also shown on the figure (upper right part) are the e-σ'_v curves followed for samples with a thickness n times larger than the thickness of a reference sample. This type of model clearly corresponds to Hypothesis B (Fig. 3).

The rheological models proposed were seldom assessed experimentally or only on the basis of the results of a few laboratory tests, generally of the same type: Constant rate of strain (CRS) tests by Crawford (1965) and Sällfors (1975); constant rate of loading tests by Burghignoli (1979); total load applied by steps by Berre & Iversen (1972) Aboshi (1973) and Larsson (1981).

Even with this abundant literature, clay behaviour did not appear clearly. The consolidation test results obtained by Berre & Iversen (1972) on specimens of different heights which are often used to validate Hypothesis B were also used by Leonards (1977) to justify Hypothesis A. The tests carried out by Aboshi (1973) on remoulded clay indicate a behaviour somewhere in between the predictions given by Hypotheses A and B. Hypothesis A previously mentioned (Fig. 3) is a strange model that would correspond to Equation (1) during primary consolidation and Equation (2) during secondary consolidation. In other words, the rheological model of the soil would depend on excess pore pressure (which however exists during both stages) rather than on effective stress, which seems to be contrary to the Terzaghi principle of effective stress.

Facing the lack of evidence concerning the rheological behaviour of soil, mostly clays, several groups of researchers from different places in the world decided to examine the problem more closely (Leroueil et al., 1985a; Mesri & Choi, 1985a and b; Larsson, 1986; Kabbaj et al., 1988; Šuklje & Majes, 1988; Magnan, 1992; Imai & Tang, 1992; Yin et al., 1994; Mesri et al., 1994 and 1995; Kim & Leroueil, 2001; Imai et al., 2005; Kobayashi et al., 2005; Mimura & Jang, 2005).

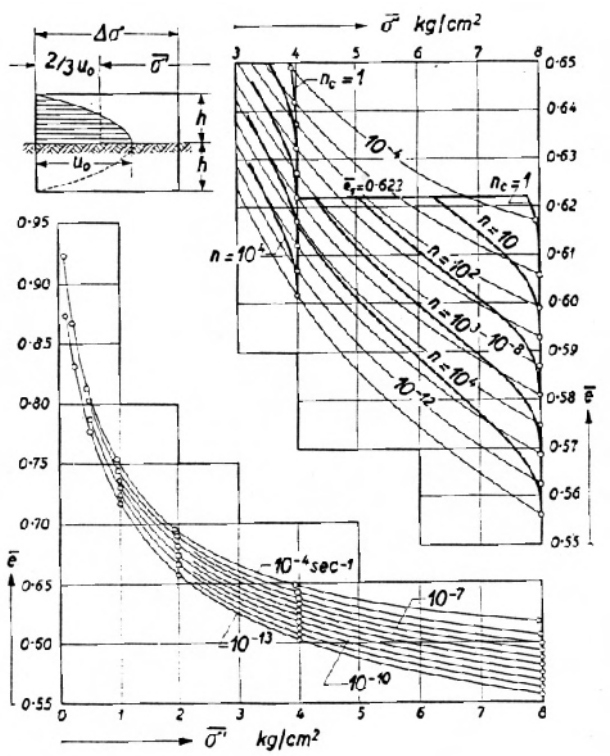

Figure 4. Isotache set for a lacustrine chalk sample (from Suklje, 1957)

The main aim of this Lecture is to summarize the experimental evidence accumulated in the last 25 years or so and to evaluate present situation. The second aim is to provide information concerning some extensions of the isotache model to multi-dimensional conditions and to include the effects of temperature.

2 LABORATORY EVIDENCE AND IMPLICATIONS

2.1 Laboratory evidence

Leroueil et al. (1983b and 1985a) performed 14 series of oedometer tests. The following tests were performed

(a) Multiple-stage loading tests with reloading at the end-of-primary consolidation ($(MSL)_p$) or after 24 h ($(MSL)_{24}$).

(b) Constant rate of strain CRS tests.

(c) Controlled Gradient tests (CGT).

(d) Long term creep tests.

At that time, long-term creep tests were performed only on Batiscan clay. However, since that time, similar series including creep tests have been performed on Berthierville and St-Alban clays (Kabbaj, 1985; Boudali et al., 1994).

Since the aim of the study was to determine the rheological behaviour of natural clays, it was first necessary to analyse the possible influence of the rate of increase of the vertical effective stress, $\dot{\sigma}'_v$. To do so, it was decided to carry out on Batiscan clay, CRS tests in which there is a constant $\dot{e} = \delta\varepsilon_v/\delta t$ and a continuous increase in σ'_v, and creep tests in which σ'_v is constant and thus $\dot{\sigma}'_v = \delta\sigma'_v/\delta t$ is equal to zero after the end of pore pressure dissipation.

Eighteen CRS tests were performed on Batiscan clay with strain rate varying from 1.7×10^{-8} s^{-1} and 4×10^{-5} s^{-1}. Typical results are presented in Fig. 5. It can be seen that:

- the higher the strain rate, the higher the pore pressure increase at the base of the specimen and, for strain rates lower than 5×10^{-7} s^{-1}, the excess pore pressure is extremely small;
- at a given strain, the higher the strain rate, the higher the effective stress or, under a given effective stress, the smaller the strain rate, the larger the strain;
- for the lower strain rate (1.7×10^{-8} s^{-1}), the compression curve intersects the other curves. This latter aspect is discussed in Section 2.3.2.

The behaviour observed in CRS tests, is very similar to that observed by Sällfors (1975) on Swedish clays. It shows in particular that in these tests where there may be excess pore pressures, the compression curve followed depends on strain rate, which is at variance with the concepts underlying Hypothesis A (Fig. 3).

Nine creep oedometer tests were performed for more than 70 days on Batiscan clay. From the results, it was possible to define effective stress-strain relations for different strain rates between 10^{-6} and 10^{-9} s^{-1}. It could be seen that this set of curves was very similar in shape and position to the ones observed in CRS tests (Fig. 5). This was thus showing that $\dot{\sigma}'_v$ has no significant influence on soil behaviour, which is thus controlled by a unique effective stress-strain-strain rate model (Equation 4; $R'(\sigma'_v, \varepsilon, \dot{\varepsilon}) = 0$). Such a result has since been confirmed by similar tests performed on Berthierville and St-Alban clays (Kabbaj, 1985).

From the results presented by Leroueil et al. (1985a), it was also observed that the $R'(\sigma'_v, \varepsilon_v, \dot{\varepsilon}_v) = 0$ relationship could be described by two curves. The first one shows the preconsolidation pressure as a function of strain rate:

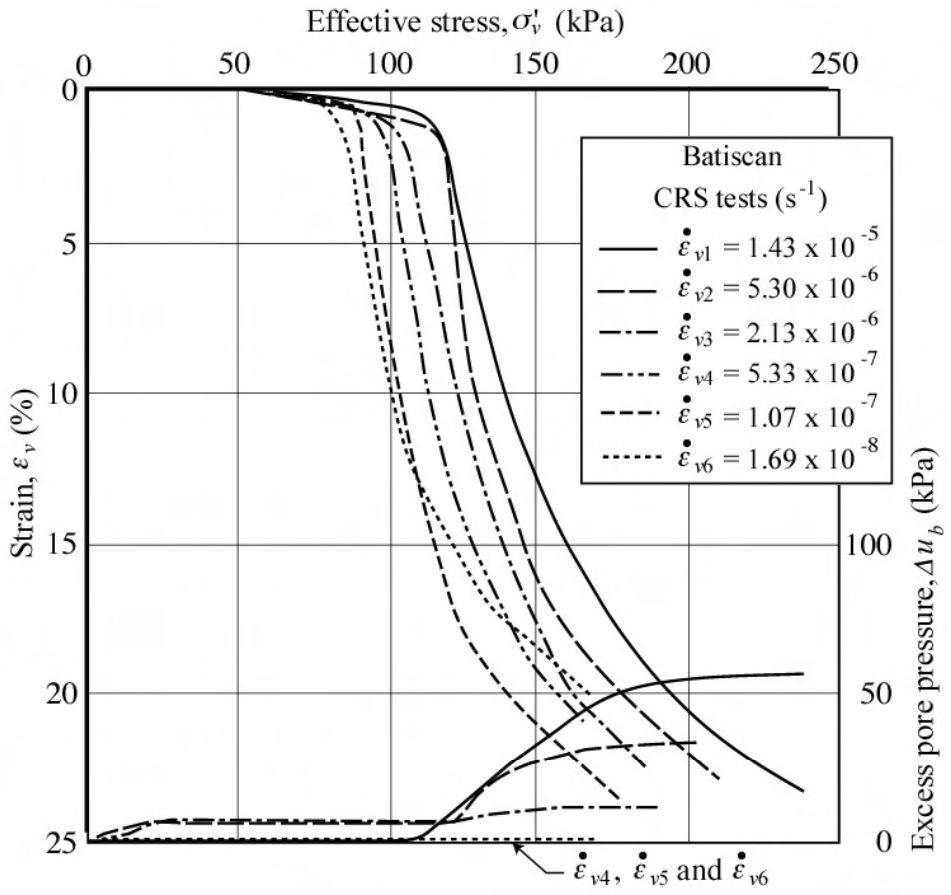

Figure 5. Typical CRS oedometer tests on Batiscan clay (from Leroueil *et al.*, 1985a)

$$\sigma'_p = f(\dot{\varepsilon}_v) \quad (6)$$

It could also be the variation of the vertical effective stress at any void ratio as a function of strain rate.

The second one shows the vertical effective stress, normalized with respect to the preconsolidation pressure associated with strain rate, as a function of strain:

$$\sigma'_v/\sigma'_p(\dot{\varepsilon}_v) = g(\varepsilon_v) \quad (7)$$

Equations 6 and 7 imply that the compression index C_c may vary with void ratio, but is independent of strain rate.

Figure 6a presents log σ'_p as a function of log ($\dot{\varepsilon}_v$) for Batiscan clay. It can be seen that the relationship is essentially linear with a slope $\alpha = \Delta \log \sigma'_p/\Delta \log \dot{\varepsilon}_v$ equal to 0.048.

The $\sigma'_v/\sigma'_p(\dot{\varepsilon}_v)$ ratios were plotted against ε_v for the 18 CRS tests (Fig. 6b). Fourteen normalized curves for strain rates between 1.4×10^{-5} and 1.07×10^{-7} s^{-1} fall in a narrow range, while four are out of this range. It was thought that the two more rapid tests carried out at a strain rate of 4×10^{-5} s^{-1} were out of the range because of high excess pore pressures; as for the two slowest tests carried out at strain rates of 3.6 and 1.7×10^{-8} s^{-1}, it was thought that they came out of the range at strains in excess of 17% mostly because of the development of microstructure (see Section 2.3.2).

Considering now the creep tests (Fig. 6c), all the normalized data fall within the range obtained from the 14 CRS tests. It can thus be concluded that for Batiscan clay, with the exception of the CRS tests performed at high strain rates, for which the pore pressures were too high, and those carried out at slow strain rates when at large strains, there is a unique effective stress-strain-strain rate relationship that can be described by two curves.

The description of the viscous behaviour of clays by 2 curves (Equations 6 and 7) has been confirmed on other clays from eastern Canada and Sweden (Leroueil et al., 1985a; Kabbaj, 1985). The case of Berthierville clay is shown in Fig. 29.

Several remarks can be made:

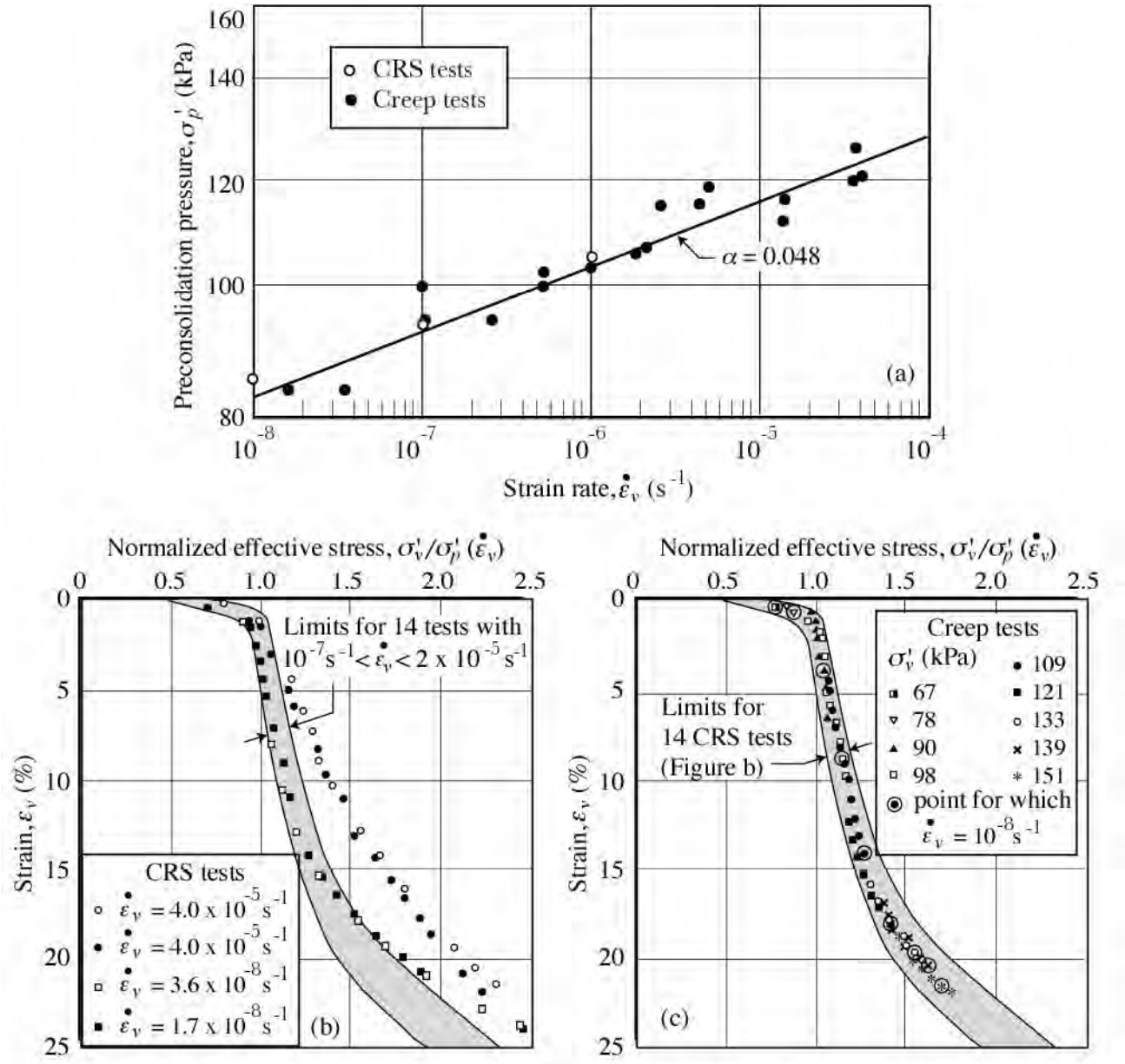

Figure 6. Rheological behaviour of Batiscan clay (7.3 m): (a) Variation of preconsolidation pressure with strain rate; (b) and (c) Normalized effective stress-strain curves deduced from CRS tests and creep tests respectively (after Leroueil *et al.*, 1985a)

- It can be easily demonstrated that α, equal to $\Delta \log \sigma'_p / \Delta \log \dot{\varepsilon}_v$, is equal to $C_{\alpha e}/C_c$:

$$\alpha = C_{\alpha e}/C_c \qquad (8)$$

This means that α should vary with the type of soil as indicated in Table 1. This also means that the preconsolidation pressure or the vertical effective stress at any strain or void ratio varies by 7 to 12%, typically by 10%, per log cycle of strain rate for inorganic clays (Table 1). It is more important in organic soils, and less important in granular soils.

- Equation (6) can thus be written:

$$\log \sigma'_p = A + \alpha \log \dot{\varepsilon}_v \qquad (9)$$

Because α takes the same value for a given type of soil, there is no doubt that Equation 9 reflects some fundamental law of physics.

- If Equation 9 reflects some universal law, Equation 7 is like the "finger print" of the considered soil. Figure 7 presents the normalized effective stress-strain curves for the Joliette and Louiseville

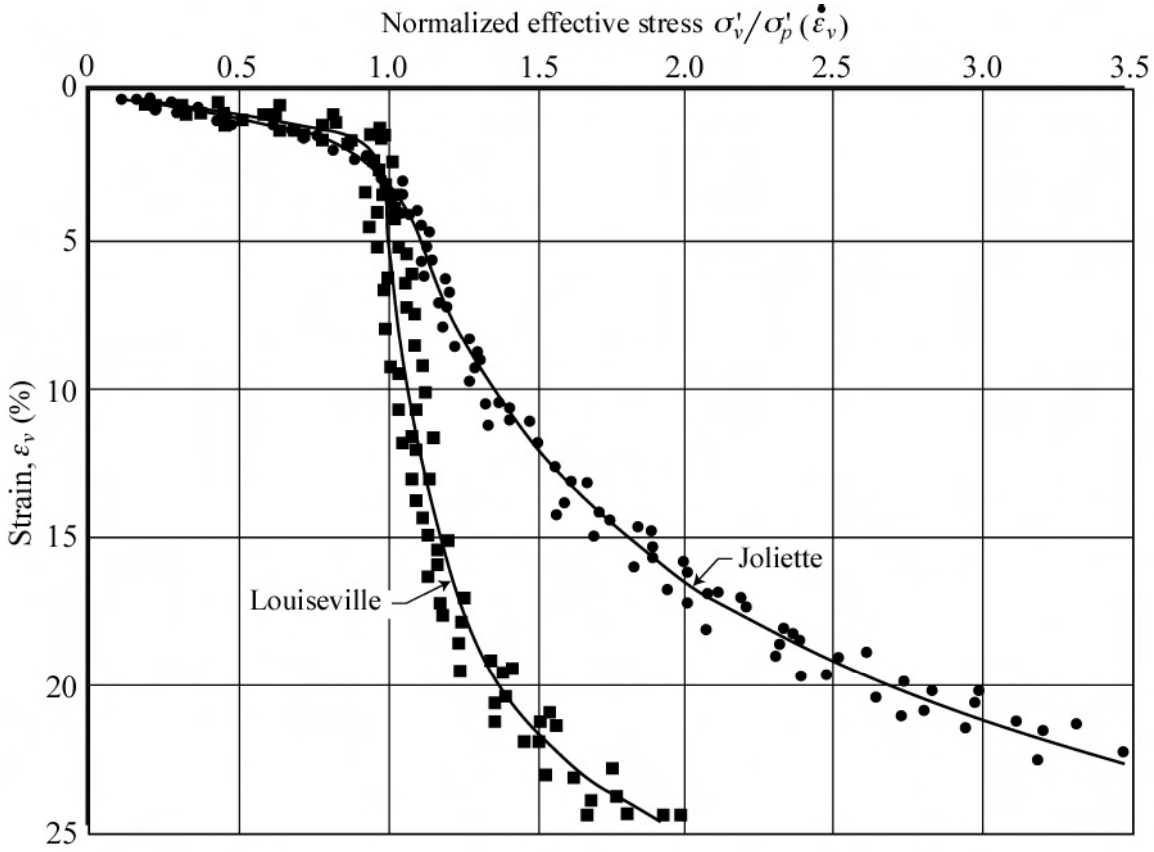

Figure 7. Normalized effective stress-strain curves for two eastern Canada clays (after Leroueil *et al.*, 1985a)

clays from Québec. It indicates that, for Joliette clay, the vertical effective stress should be equal to 2.7 times the preconsolidation pressure to reach a vertical strain of 20% whereas it has only to reach 1.35 times the preconsolidation pressure to reach the same strain for Louiseville clay.

Mesri & Feng (1986) and Mesri et al. (1995) performed special compression tests in which they put four 125 mm long sub-elements connected in series. The 4 sub-elements were isotropically consolidated (with one-dimensional drainage) whereas the axial strain of the sub-elements and the pore pressure in between were monitored. The results presented by these authors were respectively reinterpreted by Leroueil et al. (1986) and Leroueil & Marques (1996) to define the compression curves followed in the different sub-elements of the 500 mm thick layer. Figure 8 presents such compression curves followed during primary consolidation by St-Hilaire clay subjected to a pressure increment from 97 to 138 kPa. The compression curves are drawn from I (initial condition) to P (close to the end-of-primary consolidation). Also drawn on the figure is a fictitious secondary consolidation phase (PF) corresponding to $C_{\alpha e}/C_c$ (= α) = 0.03, as indicated in Fig. 2 for St-Hilaire clay. It can be seen that the compression curve followed during primary consolidation varies with the location of the sub-elements. Near the drainage boundary (sub-specimen 1), the strain rate is very high during the early stages of consolidation and, as a result, the effective stress goes to isotaches associated with high strain rates. On the other hand, for the sub-elements that are far from the drainage boundary (sub-elements 3 and 4), the strain rates are much smaller during the same period and the effective stress remains close to isotaches associated with these strain rates. However, when the soil is approaching the end-of-primary (point P), the strain rate becomes more uniform in the entire specimen and the compression curves of the sub-elements converge. After the end-of-primary consolidation, the entire specimen would be in secondary consolidation and would settle from P to F. Imai & Tang (1992) observed similar behaviour in a consolidating clay layer consisting of 7 sub-specimens in series.

The test results presented by Mesri et al. (1995) allowed the determination of the complete set of isotaches for the St-Hilaire clay. The fol-

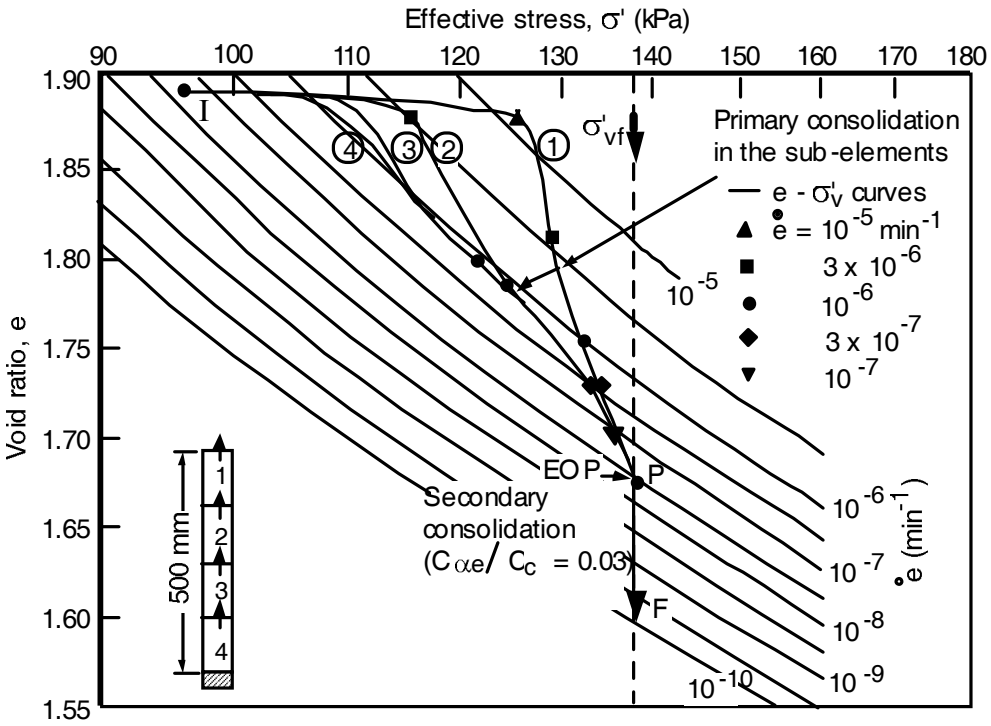

Figure 8. Consolidation of the Saint-Hilaire clay for pressure increment from 97 kPa to 138 kPa (after Mesri *et al.*, 1995; from Leroueil & Marques, 1996)

lowing comments can be made: (a) this set of isotaches coincides very well with the observed behaviour; (b) for rates between 10^{-6} and 3 x 10^{-8} min^{-1}, thus during the primary consolidation phase, the spacing between the isotaches corresponds to the $C_{\alpha e}/C_c = \alpha$ value of 0.03 observed during the secondary consolidation phase (see Fig. 2), indicating that the clay does not make any distinction between primary and secondary consolidation; (c) at rates larger than 10^{-6} min^{-1}, the variation of the effective stress per log cycle is larger than that associated with an $\alpha = C_{\alpha e}/C_c$ value of 0.03, indicating that $C_{\alpha e}/C_c = \alpha$ is possibly not a constant independent of strain rate. This aspect is further discussed in relation with field observations (Section 3.1, Fig. 18).

These results demonstrate that clay behaviour is strain rate dependent during primary consolidation and during secondary consolidation. However, according to Mesri and co-workers, and Hypothesis A, as a miracle, the end-of-primary consolidation would be independent of strain rate. This author thinks that this does not make any sense.

Mesri & Choi (1985b) and Mesri et al. (1995) compared end-of-primary compression curves obtained on specimens of different heights and concluded that they were identical and that, consequently, Hypothesis A is valid. Comparisons are shown in Fig. 9. Again, as previously indicated, it is not clear why the behaviour would be strain rate dependent during primary and secondary consolidations and not at the end-of-primary. Leroueil et al. (1985b) argued that the difference in void ratio expected in case Hypothesis B would be valid is small (about 0.060 for the Batiscan and St-Hilaire cases presented in Fig. 9) and difficult to observe experimentally; would there be development of microstructure at very small strain rates, as discussed in Section 2.3.2?

2.2 Some implications of the isotache model

Strain rate effects have some implications that are described below:

- As shown in Fig. 10, if strain rate is changed during CRS oedometer tests, soil conditions move from one isotache to another.

- Assuming that primary consolidation is completed before 24 hours in $(MSL)_{24}$ oedometer tests, the strain rate at the end of the loading periods, which can be associated with the 24-hrs compression curve is approximately equal to 2 x

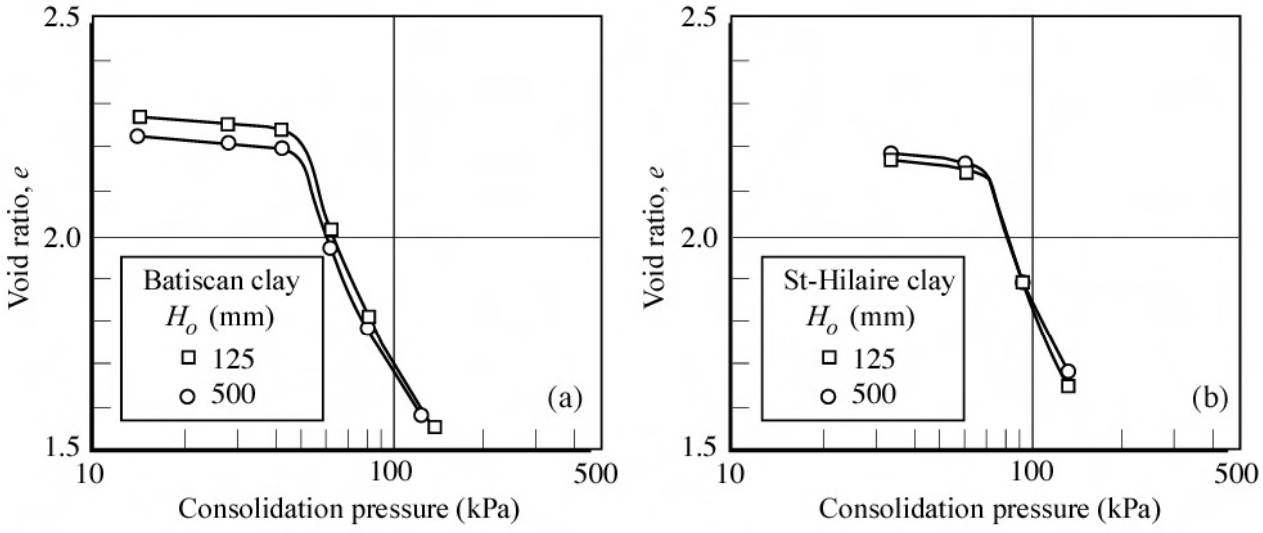

Figure 9. End–of–primary e – log σ'_v curves for specimens of different heights (after Mesri *et al.*, 1995)

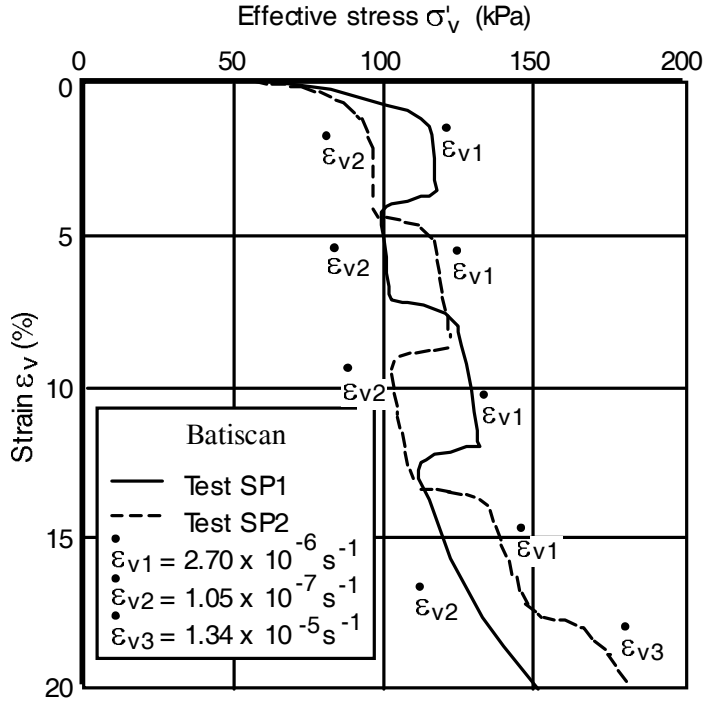

Figure 10. Special CRS oedometer tests on Batiscan clay (from Leroueil *et al.*, 1985a)

10^{-7} $C_c/(1 + e_o)$ s^{-1} for inorganic clays (Leroueil, 1988). It is thus in the order of 5 x 10^{-8} s^{-1} for low compressibility clays and 10^{-7} s^{-1} for highly compressible clays. This is smaller than the strain rates between 1 and 4 x 10^{-6} s^{-1} generally used in CRS tests. As a result, the preconsolidation pressure and the effective stress at any strain or void ratio measured in CRS tests are larger than those measured in conventional 24-hrs oedometer tes. An example is shown in Fig. 11. A compilation made by Leroueil (1996) for a variety of clays from different countries indicates a ratio $\sigma'_{p\ CRS} / \sigma'_{pconv}$ typically equal to 1.25.

- When a soil specimen is instantaneously-loaded, the strain rate is high during the early stages of consolidation and, consequently, the effective stresses go to isotaches corresponding to these high strain rates. However, with time, consolidation progresses and the strain rate decreases. As a result, the effective stress-strain condition of the soil moves towards isotaches corresponding to lower strain rates. It follows that in multiple stage loading tests, the effective stress-strain relation-

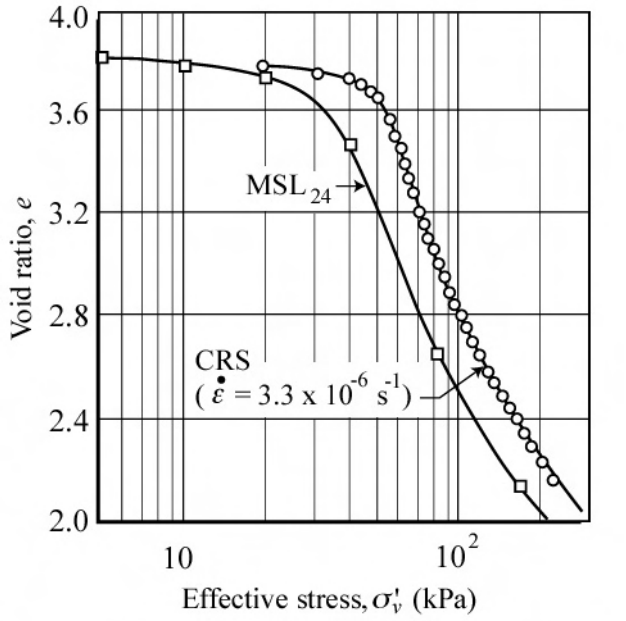

Figure 11. Comparison between stress-strain curves obtained in conventional 24 h and in CRS oedometer tests (from Hanzawa, 1989)

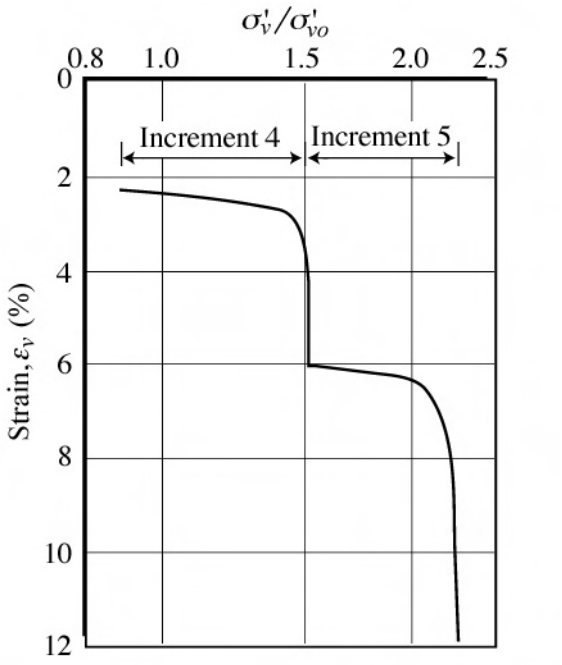

Figure 12. Multiple-stage loading test performed on Drammen clay (after Berre & Iversen, 1972)

ship really followed consists in a succession of steps as shown in Fig. 12. The behaviour shown in Fig. 8 results from the same phenomenon.

2.3 Limitations of the isotache model

2.3.1 The isotache model should be described in terms of plastic strains.

While the isotache model accurately describes the behaviour of clays when the strain is increasing, it is not the case when the axial strain remains constant, as in relaxation tests. Yoshikuni et al. (1994 and 1995) performed special oedometer tests with different phases of consolidation (opened drainage) and relaxation (closed drainage) in order to demonstrate that "consolidation is a combined process of (pore pressure) generation due to stress relaxation and dissipation due to drainage, even under constant load". In one series of three tests, these authors stopped secondary consolidation under an effective stress of 314 kPa by closing the drainage and measured the excess pore pressure. As shown in Fig. 13, the higher the strain rate at which secondary consolidation is stopped, the higher is the generated excess pore pressure, indicating that, when the strain rate decreases, the tendency to creep also decreases. One explanation is that the strain-rate model (Eqs. 6, 7 and 9) applies only to the plastic component of strain, so that, in relaxation tests where the total strain is constant, the increase in plastic strain ε^p associated with creep is compensated by a decrease in elastic strain ε^e, and thus a decrease in effective stress (Fig. 14).

$$\varepsilon = \varepsilon^e + \varepsilon^p = \text{constant} \tag{10}$$

and

$$\dot{\varepsilon}^e = -\dot{\varepsilon}^p \tag{11}$$

The rate of change in pore pressure $\dot{u}$ following closing of the drainage when the soil is in secondary consolidation at a strain rate $\dot{\varepsilon} = \dot{\varepsilon}^p$ (point A in Fig. 14) would be:

$$\dot{u} = \frac{2.3(1+e_0)\sigma'}{C_s}\dot{\varepsilon}^p \tag{12}$$

in which σ' is the effective stress at the time of closing drainage and C_s is the recompression index.

2.3.2 Possible conflict between viscous phenomena and tendency for microstructure development with time

Evidence of microstructure (bonding between soil particles or aggregates) has been found in a wide

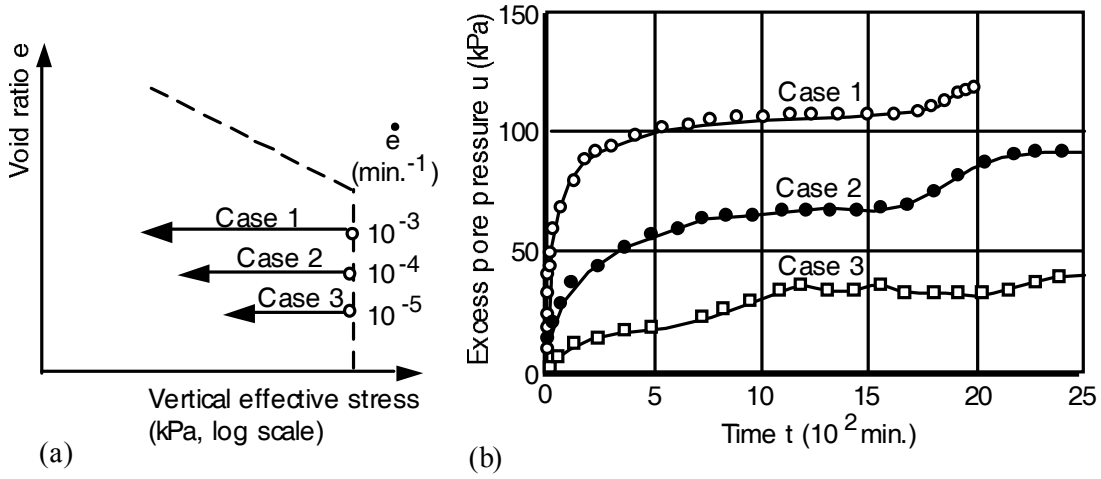

Figure 13. Excess pore pressure generation during relaxation tests under one-dimensional condition (from Yoshikuni *et al.*,1994)

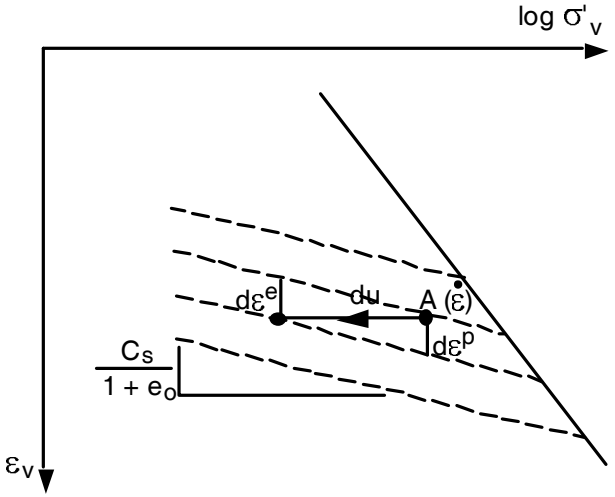

Figure 14. Strain components in relaxation test

range of natural geomaterials (see Leroueil & Vaughan, 1990). Development of microstructure with time has also been observed in some geomaterials. Leonards & Altschaeffl (1964) and Leroueil et al. (1996) showed that, in young reconstituted clays, the development of preconsolidation pressure during secondary consolidation can be much higher than that related to the decrease in void ratio. Mitchell & Solymar (1984) and Schmertmann (1991) also observed some restructuration with time in sands.

Due to their viscous behaviour, soils have a tendency to rearrange their particles and generally decrease their void ratio with time under constant effective stress. They may also be subjected to structuring phenomena that have a tendency to fix particles into position. The rate of strain determines which one of the two opposing mechanisms dominates. At relatively high strain rates, the former mechanism will dominate, as described in Section 2.1, whereas at relatively low strain rates, structuring effects may become important and modify the stress-strain-strain rate relationship. Figure 5 shows for Batiscan clay that at a strain rate of 1.7 x 10^{-8} s^{-1}, the compression curve does not fit the stress-strain-strain rate relationship developed from CRS tests performed at strain rates larger than 10^{-7} s^{-1}, crossing compression curves obtained at larger strain rates. Vaughan (1994) and Leroueil et al. (1996) present data that show a similar behaviour.

Microstructure may thus develop at low strain rates. However, the conditions that could favour the development of microstructure do not seem to be well identified yet. One important question is to know if such microstructure development that has been observed in the laboratory may also occur in in situ conditions and reduce settlements that would be expected on the basis of the isotache model?

3 FIELD EVIDENCE AND IMPLICATIONS

3.1 Field evidence

Laboratory tests provide compression curves corresponding to strain rates that are generally larger than 3 x 10^{-8} s^{-1} (Fig. 15). On the other hand, strain rates under embankments are lower than 10^{-8} s^{-1}, and generally lower than 10^{-9} s^{-1}. So, if the isotache model is valid, the vertical effective stress-strain curve followed in situ should be below the end-of-primary compression curve obtained in the laboratory, as schematised in Fig. 16.

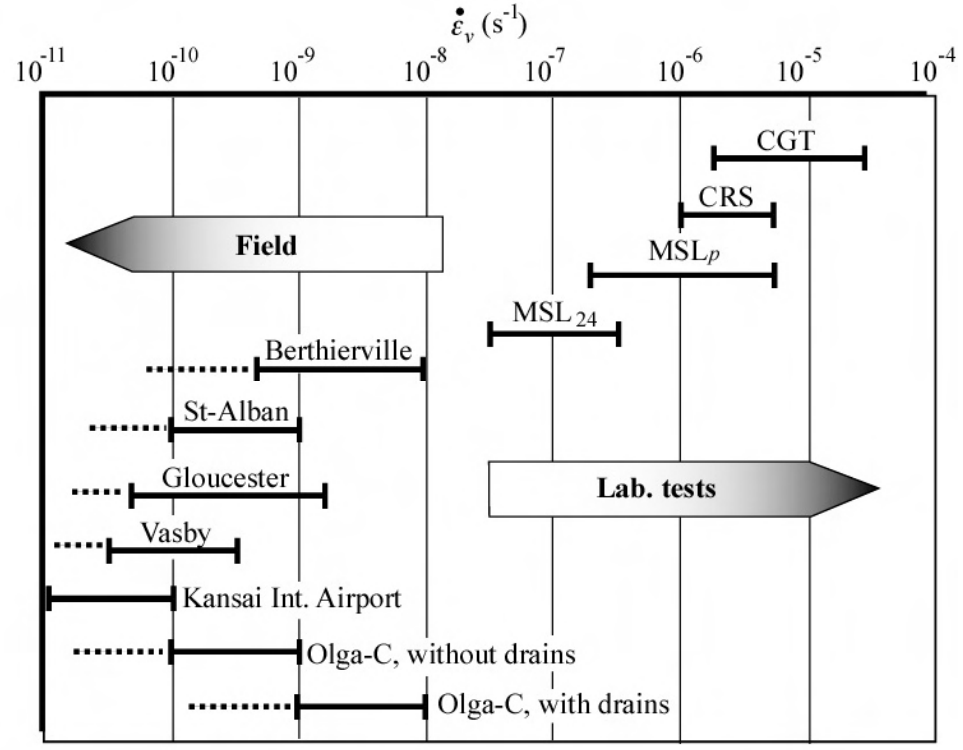

Figure 15. Ranges of strain rates encountered in laboratory tests and in situ

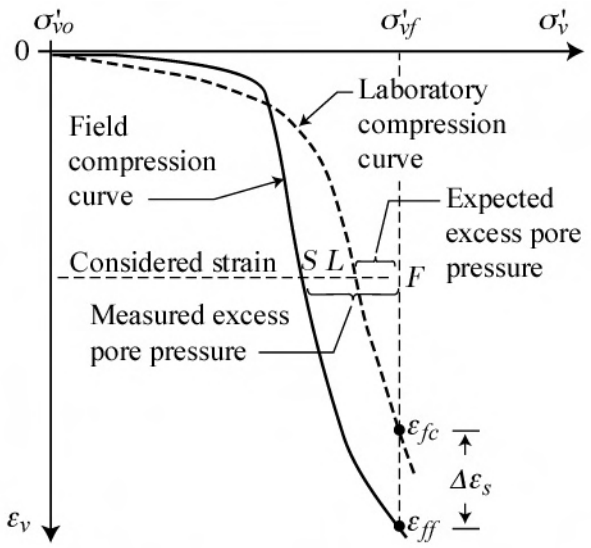

Figure 16. Typical compression curves in situ and in the laboratory

This implies that, at the same strain in the laboratory and in situ, the field pore pressure (SF in Fig. 16) is larger than the one predicted from laboratory test results (LF in Fig. 16). This also implies that at the end-of-primary consolidation, the in situ strain (ε_{ff} in Fig. 16) is larger than the laboratory one (ε_{fc} in Fig. 16).

In order to validate that later point, Kabbaj et al. (1988) examined the performance of four well documented embankments built on clay deposits in Canada (Berthierville, St-Alban and Gloucester) and in Sweden (Väsby). The 28.8 m diameter Berthierville embankment was built over a 3.2 m thick silty clay layer sandwiched between two sand layers specifically for that purpose. In each case, in situ vertical effective stress-strain curves of well-defined clay sublayers were determined on the basis of deep settlement and pore pressure measurements. They were then compared with laboratory compression curves obtained from $(MSL)_p$ and $(MSL)_{24}$ oedometer tests. For the cases of Berthierville, St-Alban and Väsby, the oedometer tests were carried out on samples retrieved with the 200 mm in diameter Laval sampler (La Rochelle et al., 1981), and thus of high quality.

Figure 17 shows such comparison for sublayers below the 4 test embankments. In all cases, at a given effective stress, the in situ strain (or settlement) is larger than that expected on the basis of the end-of-primary laboratory curve. This indicates that Hypothesis A is incorrect.

From laboratory test results obtained on Berthierville, St-Alban and Väsby clays, and in situ observations, Leroueil et al. (1988) defined vertical effective stress-strain rate curves at different strains. Comparison of laboratory and in situ behaviours at small strains (for example at σ'_p) may not be justified as laboratory results may be af-

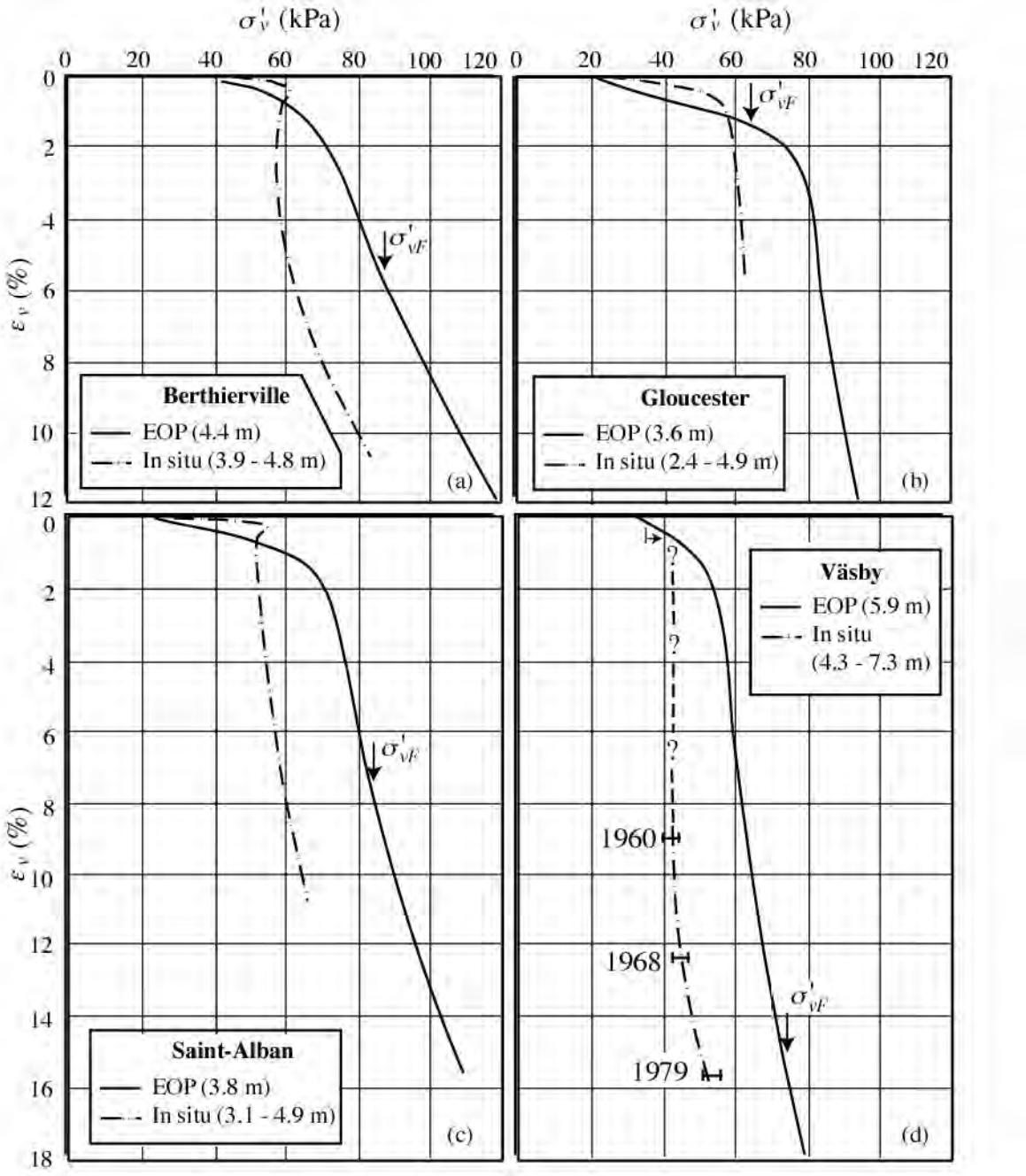

Figure 17. Comparison between stress-strain relations observed in situ and measured at end-of-primary consolidation in laboratory on four test sites (after Kabbaj *et al.*, 1988)

fected by sampling disturbance and effective stress paths followed may be quite different. Such comparison is better justified at large strains as the influence of sampling disturbance effective does not exist anymore and stress conditions are then similar in both laboratory and in situ conditions. Figure 18 shows, in a normalized manner, effective stress-strain rate relationships at a strain of 10% for four different sub-layers. Field data are in the continuity of the results obtained in the laboratory, indicating that the same isotache model applies in both laboratory and in situ conditions.

On the same figure is drawn an effective stress-strain rate relationship corresponding to α = 0.04. It fits relatively well the data points for strain rates between10^{-8} and 3 x 10^{-7} s^{-1}, range in which secondary consolidation is generally observed in the laboratory. On the other hand, Fig. 18 shows that globally, $\alpha = C_{\alpha e}/C_c$ is larger at higher strain rates and smaller at lower strain rates. This may indicate that this parameter is not

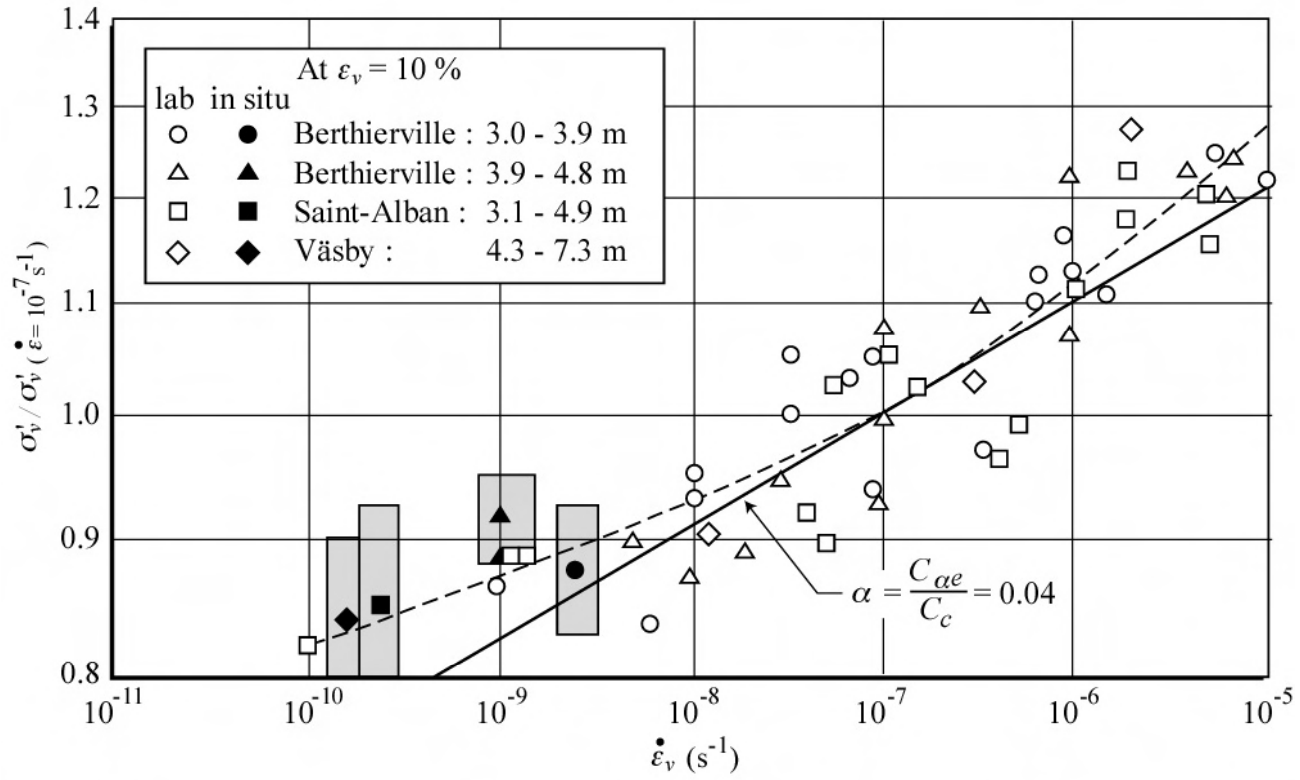

Figure 18. Normalized stress-strain rate relations at a strain of 10 % (from Leroueil *et al.*, 1988)

perfectly constant but decreases with decreasing strain rate.

At the time these studies were performed, this author was aware of the possibility of microstructuration with time of clays (see Section 2.3.2) and was prepared to find field compression curves that would not be in agreement with isotache models deduced from laboratory tests. However, Figs. 17 and 18 show that the same isotache model applies in both laboratory and in situ conditions.

It is worth mentioning that, using an elasto-visco plastic numerical model (isotache model defined in plastic strains), Kim & Leroueil (2001) were able to simulate the behaviour of multiple-stage loading, creep and relaxation oedometer tests performed on Berthierville clay as well as the in situ behaviour observed under the test embankment.

When comparing calculated and observed consolidation results, it is essential to compare both settlements (or strains) and pore pressures, indirectly effective stresses. Cases other than those previously described and in which measured and computed behaviour in terms of settlement and pore pressure had been compared have been examined, in particular by Leroueil (1988). In the 8 cases considered, a relatively good agreement was found between observed and computed settlements, in most cases by modifying the hydraulic conductivity, but in all cases except one, the measured excess pore pressures were larger than the predicted one. As schematically shown in Fig. 16, this is consistent with the effect of strain rate. This is also in agreement with experienced gained in Sweden (Larsson, 1986; Larsson & Mattsson, 2003) and in France (Magnan, 1992).

There are some cases that are worth to be examined or discussed in greater details in the context of the present Paper. This is done hereunder.

Changi Airport. The case of Changi Airport presented by Cao et al. (2001) is typical of previously mentioned observations and is worth to be described. In conjunction with a large reclamation project at Changi Airport, Singapore, a pilot test was carried out on a 294 m long and 251 m wide area. The seabed was at a depth of approximately 5.6 m. The soil deposit consists in 20-22.6 m of Upper Marine clay, 2.7 to 4.5 m of silty clay with sand, and of Lower Marine clay over a thickness of 22 to 27.3 m. The surcharge was in the order of 140 kPa. Compressibility parameters measured in the laboratory and deduced from field observations are shown in Fig. 19. They are typical of what is generally observed: σ'_p values obtained in conventional 24-hrs oedometer tests and in situ were about the same; C_r values in the field are smaller than in the laboratory, which is probably

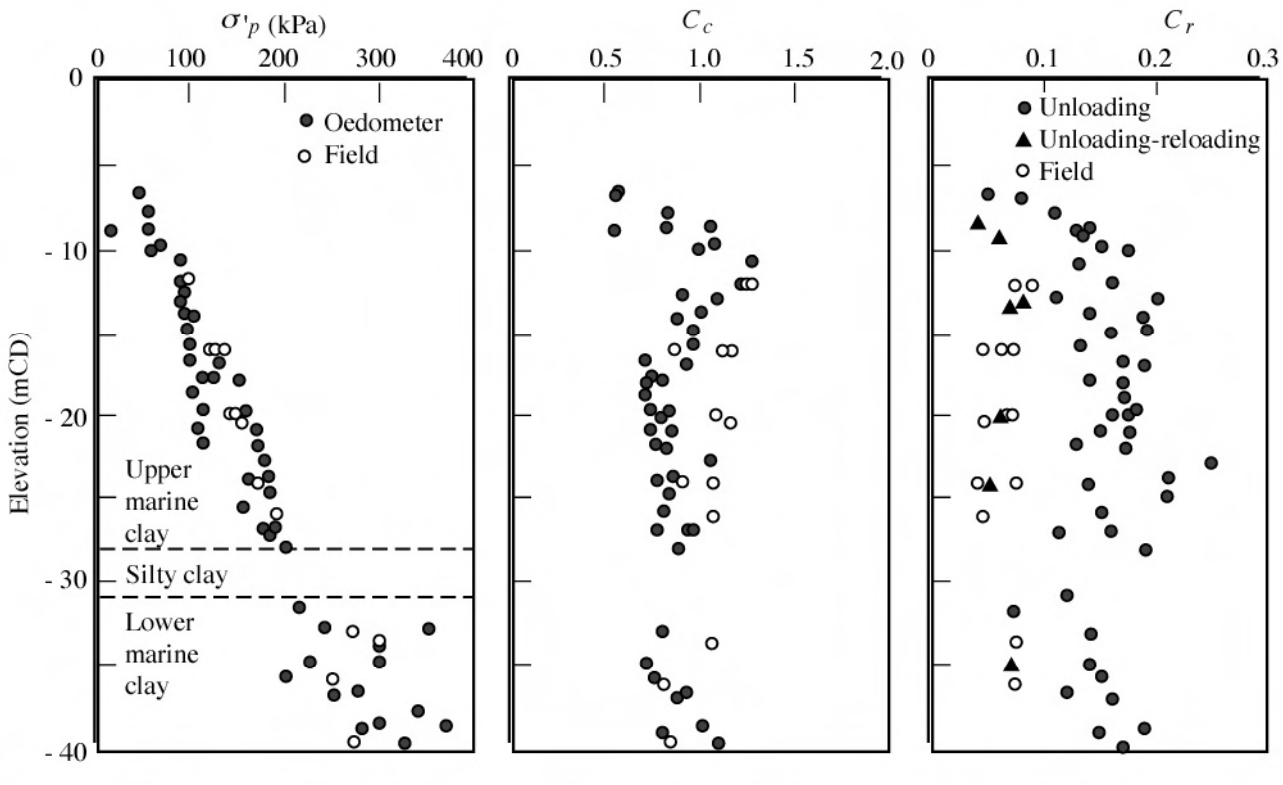

Figure 19. Comparison of preconsolidation pressures and compression parameters measured in laboratory with those back-calculated from field measurements (after Cao *et al*., 2001)

due to sampling disturbance; C_c values in the field are larger than in the laboratory, which may be also due to sampling disturbance, but also to strain rate effects.

Figure 20 shows an excellent agreement between predicted and measured settlements over the 1150 days of observation. On the other hand, the measured pore pressures were in excess of the predicted ones, by about 40 kPa at elevation -22 m (Fig. 21). This is in agreement with the strain rate effect depicted in Fig. 16.

Kansai International Airport. The case of Kansai International Airport (Phase 1) dramatically illustrates the importance of strain rate effect on settlement. The Airport is a 511 ha reclamation project 5 km offshore in Osaka Bay. Construction of the island began in 1987 and was completed in 1991; the inauguration of the Airport was in September 1994 (Arai et al., 1991; Akai & Tanaka, 1999; Akai, 2000; also see Proc. of the Symp. on Geotechnical Aspects of Kansai International Airport, 2005).

The water depth at this location was about 18m. The subsoil consists of an about 18 m of soft alluvial clay over several hundreds of metres of Pleistocene clay. These latter deposits show alternating clay and relatively thin sand or gravel layers. The overconsolidation ratio of Pleistocene clay increases with depth to reach a value of about 1.4 at a depth of 160 m. The alluvial clay layer was treated with sand drains and rapidly settled in about 6 months. The settlements observed since are due to compression of Pleistocene deposits over a thickness of about 150 m.

As evidenced in Fig. 22 from Imai et al. (2005), Kansai clays are strain rate dependent. The average α value is of 0.043, which is in the range generally observed for inorganic clays (Table 1). It can be seen, however, that a better fit between the logarithm of the normalized preconsolidation pressure and the logarithm of strain rate could be given by the dashed line, indicating again that α value may decrease with decreasing strain rate.

Figure 23 shows the measured and calculated settlements of Pleistocene deposits. The calculations were made on the basis of conventional 24-hrs oedometer test results and ignored any viscous effect during primary consolidation. At the time of the inauguration (Sept. 1994), measured and calculated settlements were about the same, at 4.50 m. Since, settlements have been larger than expected, being close to the predicted final set-

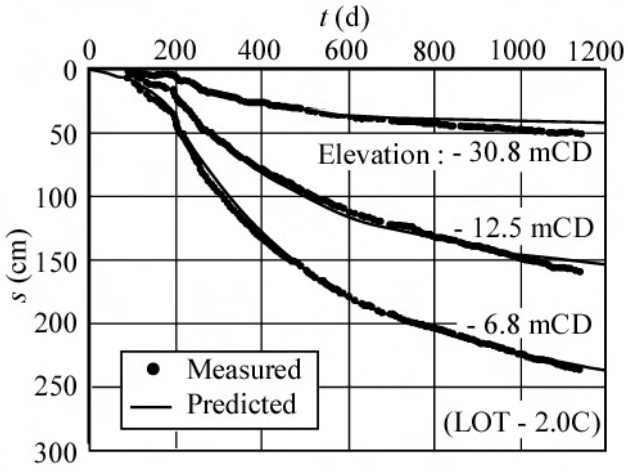

Figure 20. Comparison between measured and predicted settlements at Changi Airport site (from Cao *et al.*, 2001)

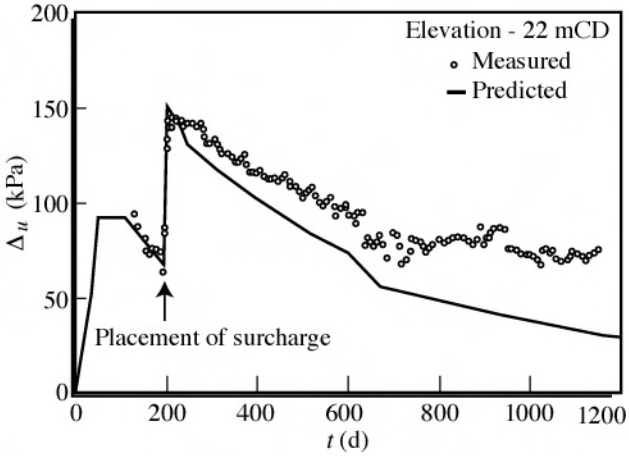

Figure 21. Comparison of measured and predicted excess pore pressures (after Cao *et al.*, 2001)

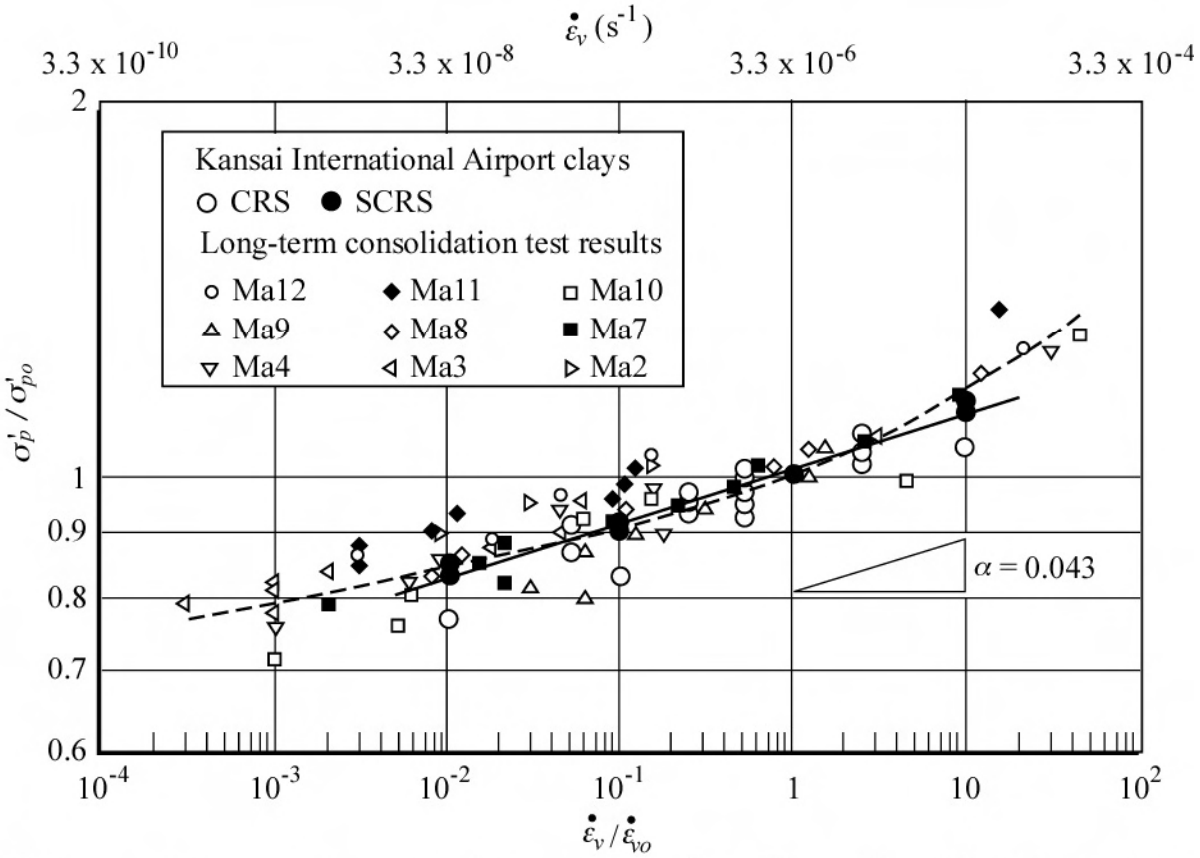

Figure 22. Strain-rate dependency of vertical yield stress for the Kansai International Airport clays (after Imai *et al.*, 2005)

tlement of 5.84 m (Akai, 2000) in 1998, and being now close to 7.0 m. The excess pore pressures measured in 1992, shortly after the end of construction, and then in 1997 and 2005, decrease only slowly and, in 2005, excess pore pressures larger than 200 kPa still exist at depths between 100 and 120 m (Fig. 24). The Pleistocene clay deposit is thus far from the end-of-primary consolidation. According to Hypothesis B and the isotache model, and considering that the average strain rate in situ is in the order of 3 x 10^{-11} s^{-1}, i.e. about 2 000 times lower than in the laboratory, such behaviour is probably not surprising.

Olga C test embankment. About 600 km north of Montreal, Hydro-Quebec built the Olga-C test

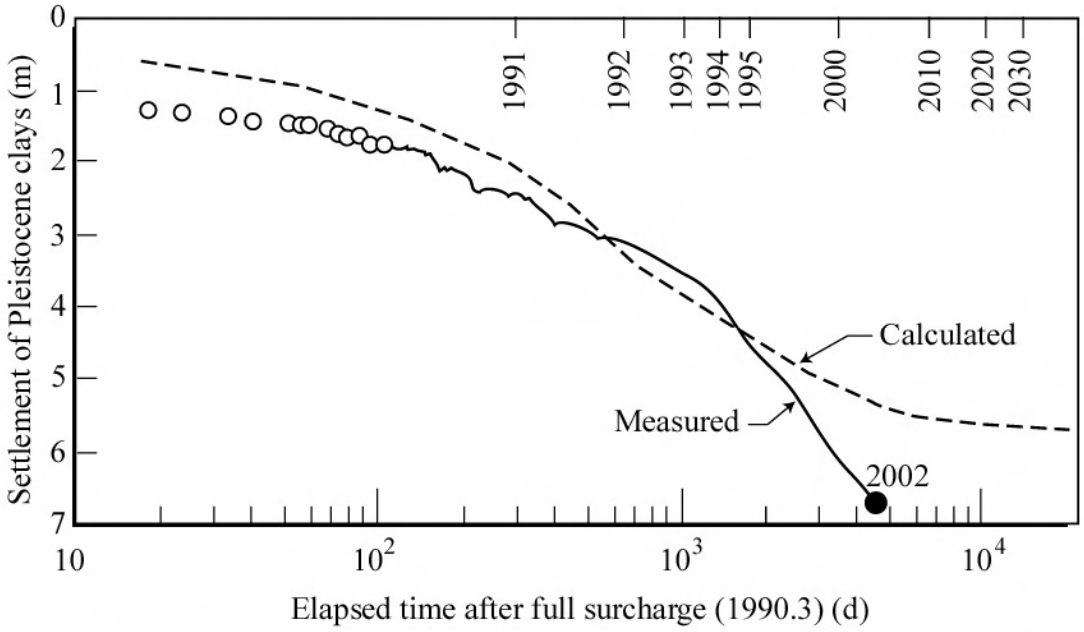

Figure 23. Calculated and measured settlement of Pleistocene clays, Kansai International Airport Island (Monitoring location Ni 2.1) (after Akai & Tanaka, 1999; from Hight & Leroueil, 2002)

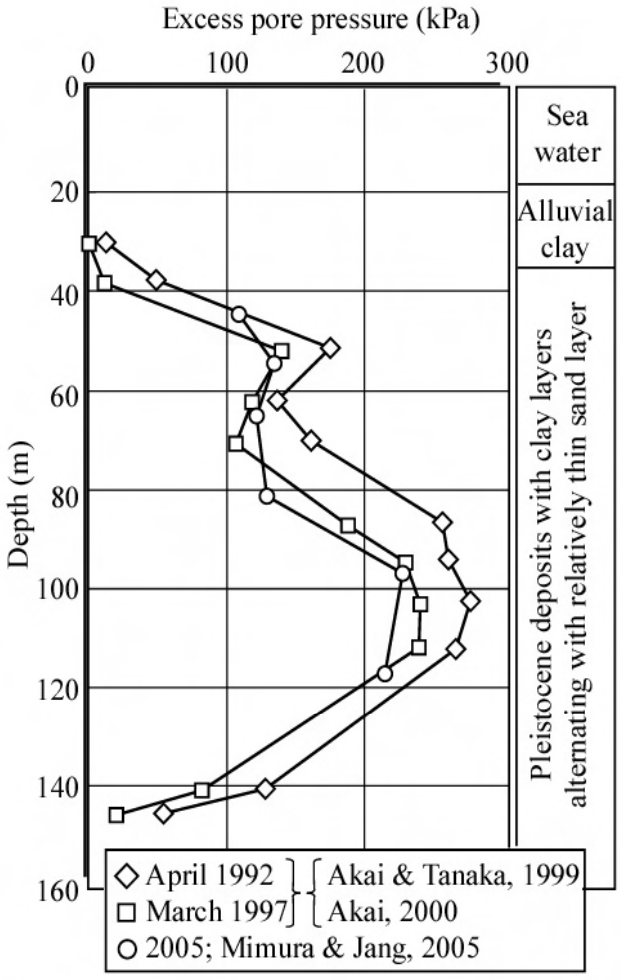

Figure 24. Excess pore pressures below Kansai International Airport Island (Monitoring location Ni 2.1) (after Akai & Tanaka, 1999; Akai, 2000; Mimura & Jang, 2005)

embankment over an about 14 m thick sensitive varved clay deposit. This embankment is 6 m high and has total width and length of 106 m and 146 m respectively. It comprises four different sections among which section A has no drain and section B has vertical drains with a spacing of 1.5 m (St-Arnaud et al., 1992; Leroueil, 1996).

Figures 25a and c respectively show the evolution with time of pore pressures observed in section A, where there are no drains, and in section B, in the middle of the grids formed by the drains. Corresponding effective stress-strain curves are shown in Figs. 25b and d. In section B where the drainage length is relatively small, the pore pressures started decreasing just after the end of construction and, consequently, the vertical effective stress was continuously increasing during the consolidation of the clay deposit. On the other hand, in section A, where the drainage length is longer, the clay mass was not able to expel the excess pore pressures generated by creep and the pore pressures continued to increase during 10-50 d after construction, before starting to decrease. Consequently, the vertical effective stress first decreased before starting to increase. The stress-strain curves followed in the two sections with different drainage lengths are thus different, and this is explained by viscous effects. This confirms the statement made by Yoshikuni et al. (1994 and 1995) that "consolidation is a combined process of (pore water) generation due to stress relaxation and dissipation due to drainage".

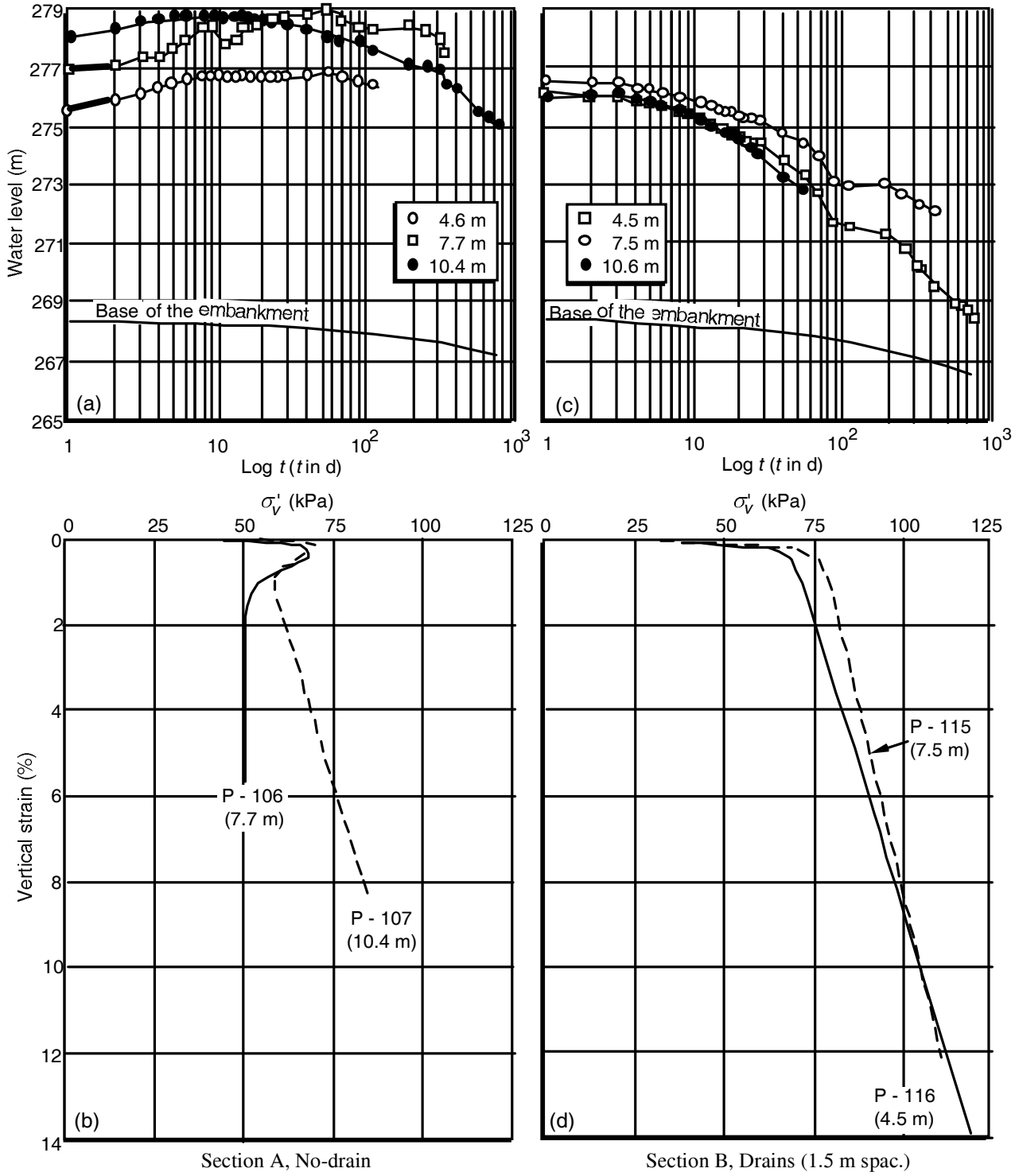

Figure 25. Olga-C test embankment (after St-Arnaud *et al*., 1992) : (a) Variation of pore pressures with time in section A, without vertical drains; (b) Appoximate stress-strain curves in section A, without vertical drains; (c) Variation of pore pressures with time in section B, with drain spacing of 1.5 m; (d) Approximate stress-strain curves in section B, with drain spacing of 1.5 m.

Similar increases in pore pressures and corresponding decreases in vertical effective stresses after the end of construction have been observed under several embankments, in particular by Crooks et al. (1984) and Kabbaj et al. (1988). Such behaviours are certainly at variance with Hypothesis A but can be explained by a viscous behaviour.

Väsby test fill. The Väsby test fill was built in 1947 by the Swedish Geotechnical Institute over 14 m of highly plastic clay. The considered test fill (without vertical drains) measured 30 m x 30 m and had a height of 2.5 m. The data collected on that site have been gathered by Chang (1981). Leroueil & Kabbaj (1987) and Kabbaj et al. (1988) examined the data and obtained the in situ compression curve shown in Fig. 17d for the sub-layer at depth between 4.3 and 7.3 m. They also performed oedometer tests on samples taken with the 200 mm in diameter Laval sampler, and the MSLp test result shown in Fig. 18d is a representative one for a specimen taken at a depth of 5.9 m. As previously indicated, the in situ compression curve is below the MSLp compression curve, confirming the effect of strain rate (also see Fig. 18).

Mesri & Choi (1985a) also examined the Väsby test fill case and found an excellent agreement between field observations and their predictions based on a unique end-of-primary compression curve. This result is at variance with the conclusion reached by Kabbaj et al. (1988). However, these predictions were established on the basis of oedometer tests carried out on specimens taken in 1967 with the 50 mm Swedish piston sampler.

Figure 26 which shows typical compression curves obtained from specimens taken at the same depth with the 50 mm and 200 mm samplers evidences sampling disturbance. This is confirmed by the overconsolidation ($\sigma'_p - \sigma'_{vo}$) associated with the end-of-primary consolidation (MSLp) tests that was estimated to 7 kPa by Mesri & Choi (1985a) on the basis of 50 mm samples and was found equal to about 20 kPa on the basis of 200 mm samples. It is clear in that case that the good agreement obtained by Mesri & Choi (1985a) results mostly from the effect of sampling disturbance compensating for strain rate effect.

This conclusion is confirmed by Larsson and Mattsson (2003) who re-analysed Väsby test fill data and found that without considering creep during primary consolidation, the settlement at the end-of-primary should have been 1.4m, and that this latter settlement was reached in 1966, whereas there were still about 30 kPa of excess pore pressures. This is in good agreement with the data presented in Fig. 17d. Larsson & Matsson (2003) added that in 2002, surface settlement was just over 2.0 m and there were still excess pore pressures with a maximum value of 12 kPa.

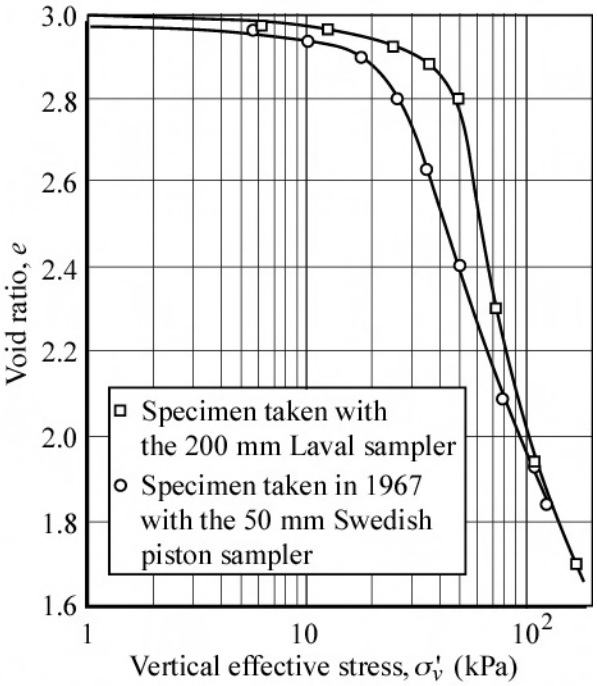

Figure 26. Typical compression curves for Väsby clay at a depth of 4.0 - 4.3 m (after Leroueil and Kabbaj, 1987)

Skå-Edeby test fills. In 1957, the Swedish Geotechnical Institute built four test fills for the construction of an airfield at Skå-Edeby. The soil on that site consisted of up to 15 m of soft clay. One of the test fills was built without vertical drains (Area IV), while vertical sand drains with different spacings were installed under the other fills.

Mesri et al. (1994) studied the Test Fill Area III. Under that test fill, 18 cm diameter displacement type sand drains were installed at 1.5 m spacing in a triangular pattern. The fill height was about 2.5 m. They found a very good agreement between observed settlements and settlements computed on the hypothesis of the same end-of-primary compression curve; they also found a relatively good agreement for pore pressures over an about two year period, while primary consolidation was not completed yet.

Larsson & Mattsson (2003) studied the nearby undrained Test Fill Area IV (1.5 m of fill; $\Delta\sigma$ = 27 kPa). They found that without considering creep during primary consolidation, the settlement at the end-of-primary should have been 0.75 m, and that this latter settlement was reached in 1972, whereas there were still about 20 kPa of excess pore pressures. This means that, 15 years after construction, there was almost no increase in vertical effective stress. In 2002, thus 45 years after construction, the settlement amounted 1.10 m

and the maximum pore pressure was of 8 kPa. This confirms that viscosity develops during primary consolidation.

It is not clear why these authors came with so different conclusions. Possible explanations are the effect of sampling disturbance, differences in strain rates, the influence of the 18 cm diameter displacement sand drains used in some areas, and different methods of analysis.

3.2 Additional remarks

All the very well documented case histories previously mentioned are showing the influence of strain rate during primary consolidation, at least when high quality samples are used for evaluating compressibility parameters. However, it has to be mentioned that Mesri et al. (1994) also compared measured and computed settlements for other embankments and found an excellent agreement.

Because of sampling disturbance, because the effective stress paths followed in the laboratory and in situ are different, and because of possible differences in strain rate and temperature, it can be difficult to conclude on rheological by comparing yield stresses (preconsolidation pressures) observed in the laboratory and in situ.

Morin et al. (1983) and Leroueil (1988) compared vertical yield stress (or preconsolidation pressure) mobilized in situ, σ'_{vy}, with preconsolidation pressures obtained in conventional 24-hrs oedometer tests, $\sigma'_{p\ conv}$. They came to the conclusion that $\sigma'_{p\ conv}$ is representative of σ'_{vy} for OCRs, estimated on the basis of $\sigma'_{p\ conv}$, between 1.2 and 2.5, may be smaller by about 10% for nearly normally consolidated clays and is larger for estimated OCRs in excess of 2.5 (see Leroueil, 1996 for further details).

Mesri et al. (1995) found an excellent agreement between vertical yield stress obtained in the field and preconsolidation pressures obtained in the laboratory at the end-of-primary consolidation, $\sigma'_{p\ EOP}$. Except for nearly normally consolidated clays (OCRs less than about 1.3), this does not correspond to this author's experience; more than that, it is thought that $\sigma'_{p\ EOP}$ measured on good quality samples could significantly overestimate the in situ vertical yield stress of overconsolidated clays (say OCRs larger than about 1.6).

3.3 Practical implications

From observations deduced from very well documented embankments and with reference with laboratory tests performed on high quality samples, it appears that the end-of-primary consolidation curve obtained in the laboratory underestimates field settlements.

One approach for estimating long term settlements is to use numerical models that incorporate viscous effects such as those developed by Adachi et al. (1982, 1996), Kabbaj et al. (1986), Szavits-Nossan (1988), Svano et al. (1991), Yin et al. (1994), Yashima et al. (1997), Rowe & Hinchberger (1998), Kim & Leroueil (2001) and others.

Leroueil et al. (1988) also suggested that a strain $\Delta\varepsilon_s$ be added to the strain estimated on the basis of the conventional 24-hrs oedometer test (which, in itself already incorporates some secondary compression) to evaluate the strain at the end of in situ primary consolidation. Simply calculated to take into account the effect of strain rate, $\Delta\varepsilon_s$ is equal to:

$$\Delta\varepsilon_s = \frac{\alpha\, C_c}{(1+e_0)}[\log 10^{-7} - \log(\dot{\varepsilon}_{EOP})] \qquad (13)$$

where $\dot{\varepsilon}_{EOP} = (0.16\ k\ u'_o/\gamma_w\ H^2)$; C_c = compression index under the final effective stress; e_o = initial void ratio; k = hydraulic conductivity of the clay; α = parameter defined in Equation 9; u'_o = initial excess pore pressure; and H = maximum drainage length.

Taking into account an α value equal to 0.03 and a temperature in the field 12°C below that of the laboratory (typical conditions for Canada and Scandinavia), Leroueil (1996) came with a slightly different equation for $\Delta\varepsilon_s$, then named $\Delta\varepsilon^*_s$, that is represented in Fig. 27. $\Delta\varepsilon^*_s$ would be about 1.3% for the Berthierville embankment, 2.5% for the St-Alban embankment, and 5.6% for the Väsby embankment.

Using Equation 13 and very coarsely estimated parameters, this author came to an estimation of settlements in addition of those calculated on the basis of $(MSL)_{24}$ tests in the order of 2.5 m for the Kansai International Airport (Letter sent to Professor H. Aboshi in 1995).

Previous calculations are valid for cases in which high quality samples are available and final

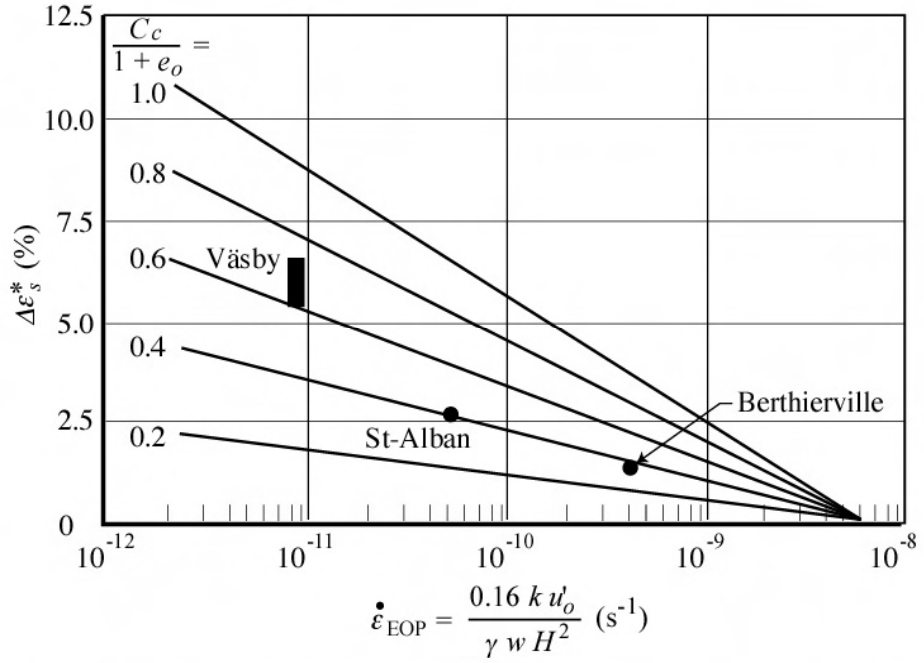

Figure 27. Estimation of the end-of-primary in situ strain $\Delta\varepsilon_s^*$ in excess of that determined from conventional 24-hrs laboratory oedometer test, when strain rate and temperature effects are considered (from Leroueil, 1996)

effective stresses are well known. This is not always the case and the following practical approach is suggested:

- In highly compressible clays [$C_c/(1 + e_o)$ values larger than 0.25] or for embankments of special importance (test embankments, embankments for which the magnitude of settlements may have important consequences), viscous effects could be significant and should be considered in the calculation of settlements at the end-of-primary consolidation.
- For usual projects in clays of low compressibility [$C_c/(1 + e_o)$ values less than 0.25], $\Delta\varepsilon^*_s$ is smaller than 2.5% and is often compensated by some disturbance of the clay samples and some reduction of the final effective stress due to settlement and a raise of the water table in the embankment. In these cases, it is thought that conventional 24-hrs oedometer test results, which already include some secondary compression, could be used without any correction to evaluate in situ end-of-primary consolidation settlement.
- When vertical drains are used to accelerate the consolidation process or when the clay deposit is thin or stratified, the strain rate at the end-of-primary consolidation is larger than 3×10^{-10} s^{-1} in most cases. Consequently, $\Delta\varepsilon^*_s$ remains relatively small and, for the same reasons as those indicated in the preceding item, it is thought that the conventional 24-hrs oedometer test results could be used without any correction for calculating settlements.

4 INFLUENCE OF TEMPERATURE

4.1 Laboratory evidence

In recent years, many studies have been conducted on the effects of temperature on the compressibility of clays (Eriksson, 1989; Tidfors & Sällfors, 1989; Boudali et al., 1994; Graham et al., 2001; Marques et al., 2004) and peats (Edil & Fox, 1994). Typical CRS test results, obtained on sulphide clay from Luleå, Sweden, are shown in Fig. 28. It can be seen that there is a significant effect of temperature on the compressibility of the clay. With increasing temperature, the soil becomes more compressible in the overconsolidated range, the preconsolidation pressure decreases, and the entire compression curve moves towards smaller effective stresses. It can also be seen on Fig. 28b that the effect is more important at temperatures below 35°C than at higher temperatures.

Boudali et al. (1994) performed CRS tests at different strain rates and temperatures on 3 clays, among which the Berthierville clay previously mentioned. Their results, summarized in Fig. 29 show the following: (a) the preconsolidation pressure, or the vertical effective stress at any void ra-

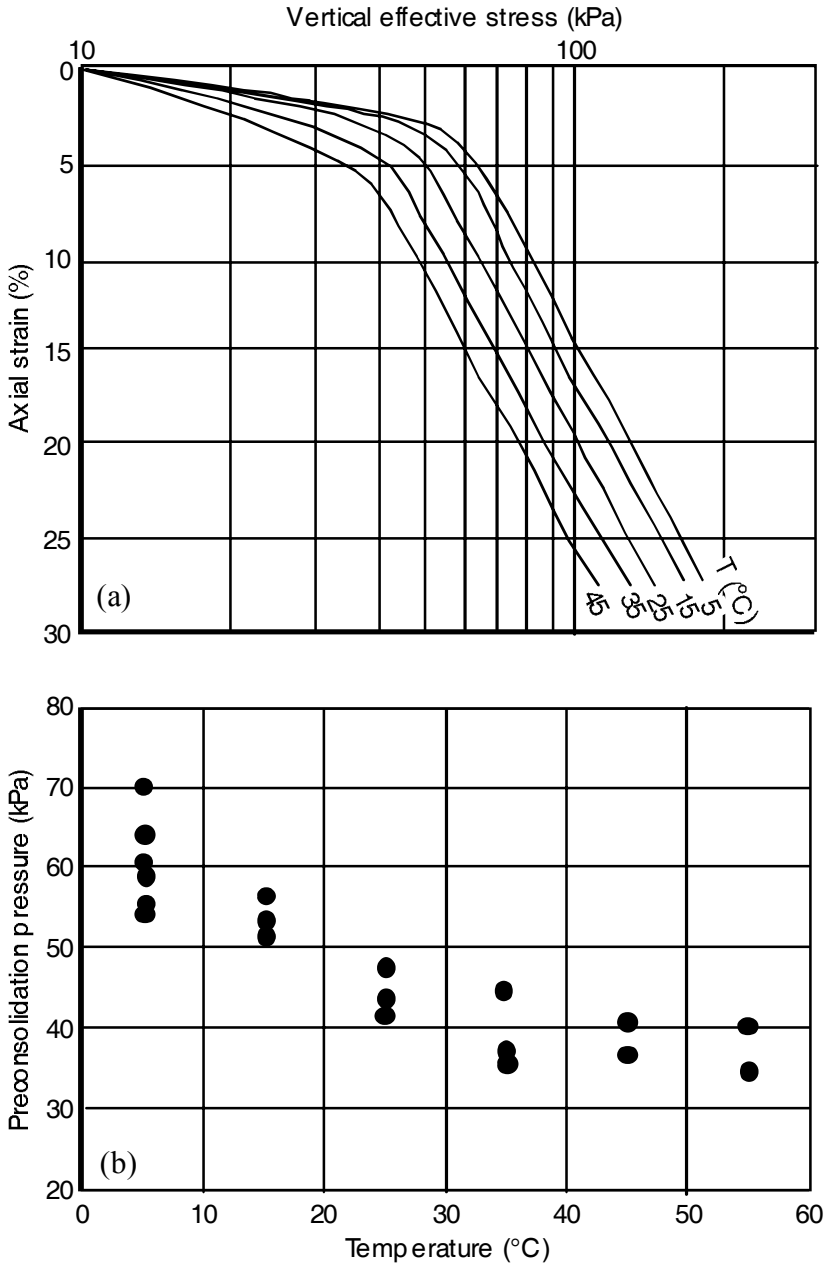

Figure 28. Oedometer tests performed on Lulea clay at various temperatures (from Eriksson, 1989)

tio, can be described as a function of strain rate and temperature (Fig. 29a); and (b) the effective stress-strain curves obtained at different strain rates and temperatures reduce to a unique one when normalized with respect to the preconsolidation pressure corresponding to the strain rate and temperature used in each test (Fig. 29b). The isotache model proposed by Leroueil et al. (1985a) and described by Equations 6, 7 and 9 can thus be extended for including temperature effects. This isotache-isotherm compression model can then be described by the following equations:

$$\sigma'_p = f(\dot{\varepsilon}_v, T) \qquad (14)$$

and

$$\sigma'_1 / \sigma'_p(\dot{\varepsilon}_v, T) = g(\varepsilon_1) \qquad (15)$$

Marques et al. (2004) found similar results for St-Roch-de-l'Achigan clay. Equations 14 and 15 imply that the compression index C_c may vary with void ratio, but is independent of strain rate and temperature.

From the experimental results obtained, it seems that $\alpha = C_{\alpha e}/C_c$ and slope of the log σ'_p – log $\dot{\varepsilon}$ relationship is not influenced by temperature (see Fig. 29a). Equation 14 can thus be written:

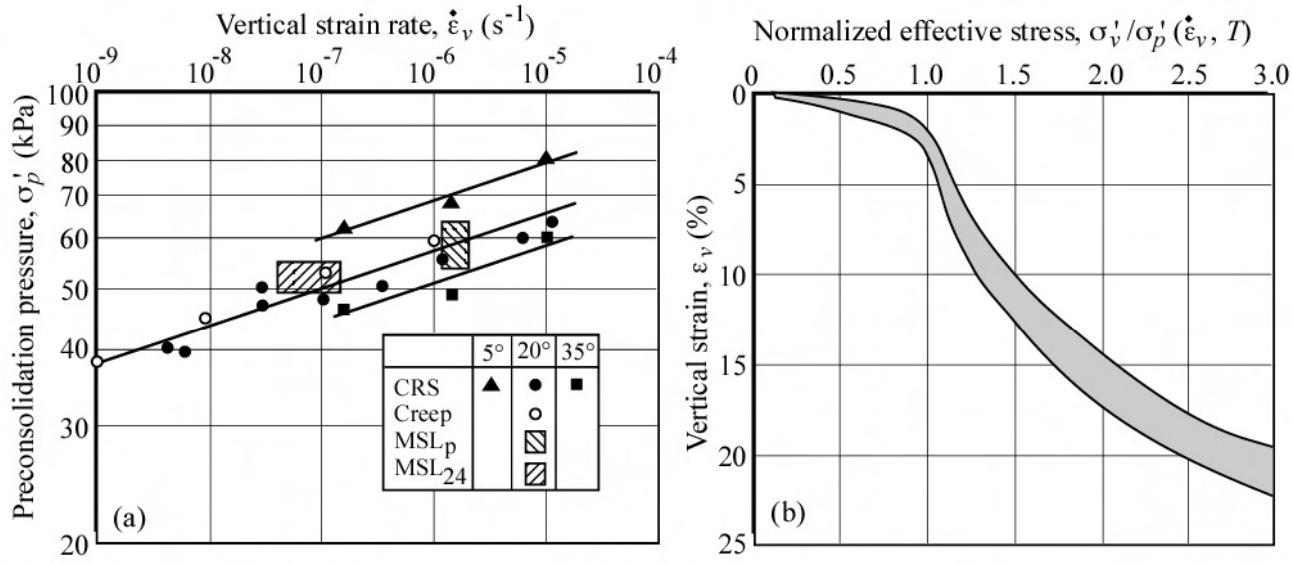

Figure 29. One-dimensional compression of Berthierville clay (from Boudali *et al.*, 1994 and Kabbaj, 1985): (a) Preconsolidation pressure as function of strain rate and temperature; and (b) Normalized effective stress-strain curve

$$\log \sigma'_p = A(T) + \alpha \log \dot{\varepsilon}_v \qquad (16)$$

Figure 30 shows, for a variety of clays, the preconsolidation pressure (or vertical effective stress at a given void ratio) normalized with respect to the preconsolidation pressure (or vertical effective stress at a given void ratio) measured at 20°C. It can be seen that the change in normalized stress with temperature is essentially the same for all the considered clays, being almost 1% per °C between 5 and 35°C, and much smaller at larger temperatures.

Moritz (1995a and b) proposed the following equation for describing the variation of the preconsolidation pressure with temperature:

$$\sigma'_{p(T)} = \sigma'_{p(To)} (T_o/T)^{\alpha} \qquad (17)$$

in which α is a soil parameter different from the α parameter in Equation 9.

Equation 17 is in fact very close to the law describing the decrease in viscosity of water with increasing temperature (Marques et al., 2004). Laloui & Cekerevac (2003) proposed the following equation:

$$\sigma'_{p(T)} = \sigma'_{p(To)} [1 - \gamma \log (T_o/T)] \qquad (18)$$

γ is a soil parameter that varies to some extent with the soil considered. It takes a value of 0.40 for the Luleå clay tested by Eriksson (1989), (Fig. 28).

The variation of the preconsolidation pressure (or of the effective stress at any void ratio or strain) with strain rate and temperature thus takes the same form in many geomaterials and obviously corresponds to a fundamental viscosity law, possibly the "rate process theory" (Murayama & Shibata, 1961; Mitchell, 1964, 1993). Again, the normalized effective stress-strain curve is like the "finger print" of the considered soil.

4.2 Implications

An implication of temperature effects is that, as shown by Marques et al., if in CRS tests, temperature is changed, the effective stress goes from one isotherm compression curve to another one.

The viscosity of clays, and the combined effect of strain rate and temperature on soil skeleton and water, can be illustrated by some test results obtained by Boudali et al. (1994) on Berthierville clay. These results, shown on Fig. 31, can be described as follows:

- The vertical strain generated by a change in temperature of 30°C, under a constant effective stress in the overconsolidated range, remains small, in the order of 0.5%.
- In the normally consolidated range, it can be seen that, at a given strain rate (10^{-5} or 1.6 x 10^{-7}

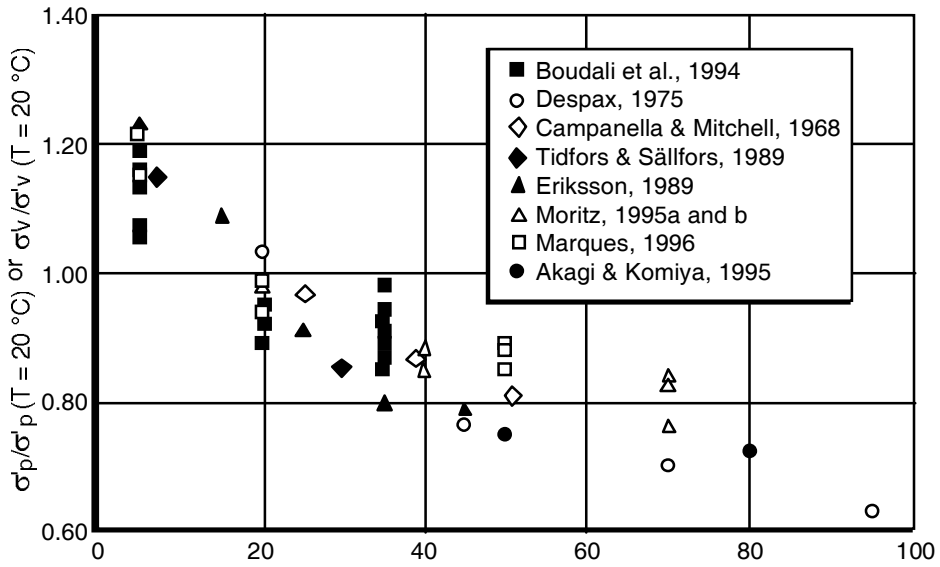

Figure 30. Variation of the normalized preconsolidation pressures, or vertical effective stress at a given void ratio, with temperature (from Leroueil & Marques, 1996)

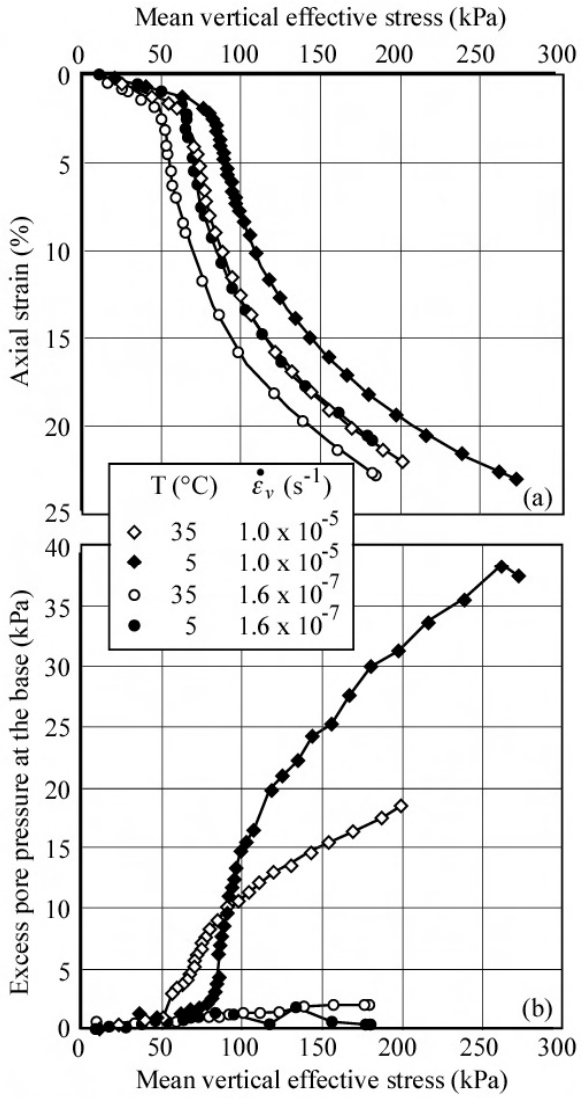

Figure 31. Typical CRS oedometer test results obtained at different strain rates and temperatures (after Boudali et al., 1994)

s^{-1}), the higher the temperature, the lower is the compression curve; also, at a given temperature (5 or 35°C), the higher the strain rate, the higher is the effective stress at a given strain. This reflects the viscosity of the soil skeleton.

-As shown on the figure, temperature effects combine with the effects of strain rate to influence the viscous behaviour of clays. For this reason, the stress-strain curves obtained at (T = 5°C and $\dot{\varepsilon}_v = 1.6 \times 10^{-7}$ s^{-1}) and at (T = 35°C and $\dot{\varepsilon}_v = 10^{-5}$ s^{-1}) coincide. This is because, as shown on Fig. 29a, the preconsolidation pressures corresponding to these two conditions are both equal to 61 kPa.

- The pore pressures at the base of the specimen shown on Fig. 31b are also of interest. At a strain rate of 1.6×10^{-7} s^{-1}, the generated excess pore pressures remain very small through the entire tests. It is not the case at a strain rate of 10^{-5} s^{-1}. The excess pore pressures at this strain rate remain small in the overconsolidated range, where c_v is relatively large, and start increasing at the preconsolidation pressure, when the soil becomes normally consolidated and c_v is much lower. For this reason, the pore pressure starts increasing at an effective stress of about 60 kPa at 35°C and of about 80 kPa at 5°C. This results from the effect of temperature on soil skeleton. In the normally consolidated range, the excess pore pressure observed at 5°C becomes larger than that at 35°C, which results from the fact that water viscosity is smaller at 35°C than at 5°C, and consequently the hydraulic conductivity is larger. This results from the effect of temperature on water hydraulic conductivity.

Temperature also has field applications: preloading of soft soil deposits by heating (Miliziano, 1992; Edil & Fox, 1994; Marques & Leroueil, 2005); energy storage in soft soil deposits (Moritz, 1995a and b); radioactive waste disposal (Houston et al., 1985; Hueckel and Peano, 1987; Lingnau et al., 1995).

4.3 Limitations of the isotache-isotherm model

It has been indicated in Sections 2.3.2 that, at least in some soils, microstructure may develop at low strain rates. Performing CRS tests at different strain rates and temperatures, Marques et al. (2004) observed that microstructuring becomes more important when temperature increases from 10°C to 50°C. The isotache-isotherm model may thus deteriorate under some strain rate and temperature conditions.

5 SOME ASPECTS OF GENERAL BEHAVIOUR

5.1 Influence of strain rate and temperature on the general behaviour of soils

5.1.1 Limit state curve

Shear tests performed on clays have shown that the peak strength envelope is strain rate dependent in the overconsolidated domain (Lo & Morin, 1972; Tavenas et al., 1978; Leroueil & Marques, 1996). Test results obtained on Lower Cromer till (Hight et al., 1987) and on Boston Blue clay (Sheahan et al., 1996) indicate that this may not be general. However, the preconsolidation pressure and the entire limit state curve, at least below the critical state envelope, is strain rate dependent. This has been clearly shown by Boudali (1995) for Berthierville clay (Fig. 32a) and by Leroueil & Marques (1996) for Mascouche clay.

Boudali (1995) also showed that, at a given strain rate, the limit state curve is temperature dependent (Fig. 32b). Burghignoli & Desideri (1988) on reconstituted Todi clay, Graham et al. (2001) on illite and Marques et al. (2004) on St-Roch-de-l'Achigan clay observed similar effects of temperature. Figure 33 summarizes test results obtained by Marques et al. (2004). Below the critical state line, the effect of temperature is very clear. As for the peak strength envelopes, that at 10°C is the highest; on the other hand, those at 20°C and 50°C do not show a clear effect of temperature. This could be due: (a) as suggested by Hueckel & Baldi (1990), to a combined result of weakening of the interparticle contacts and strengthening of the soil due to a decrease in void ratio when the soil is heated from 20°C to 50°C; (b) to microstructuring of the clay when the soil is

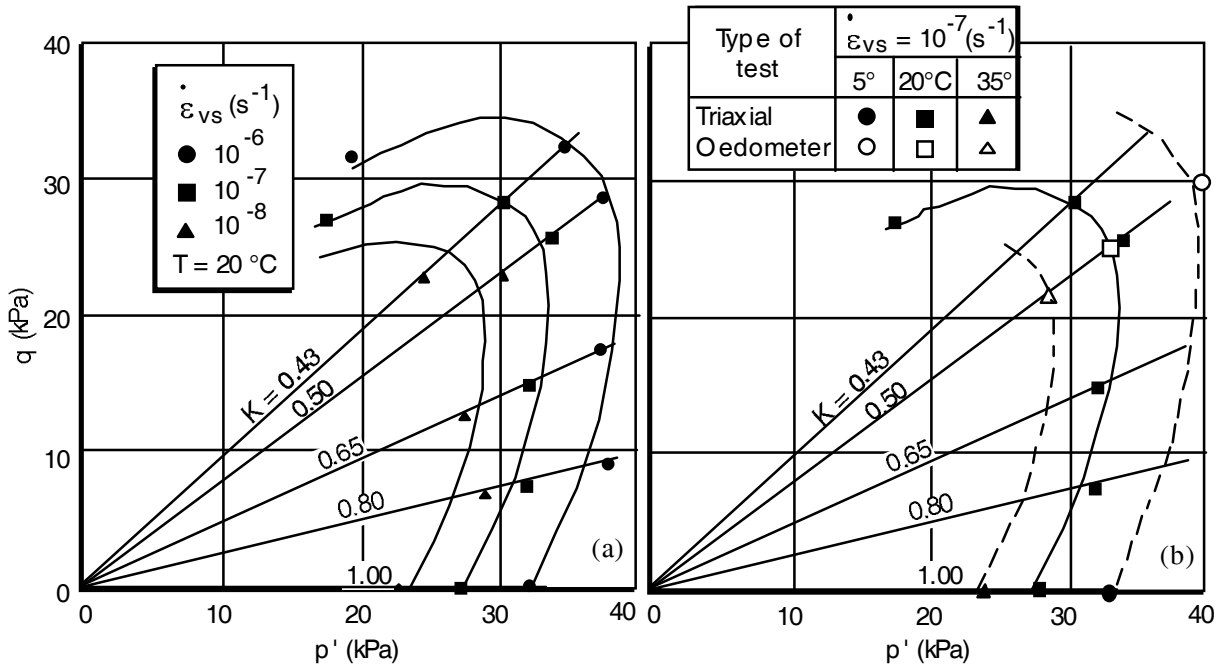

Figure 32. Variation of the limit state curve of Berthierville clay with (a) strain rate and (b) temperature (after Boudali,1995)

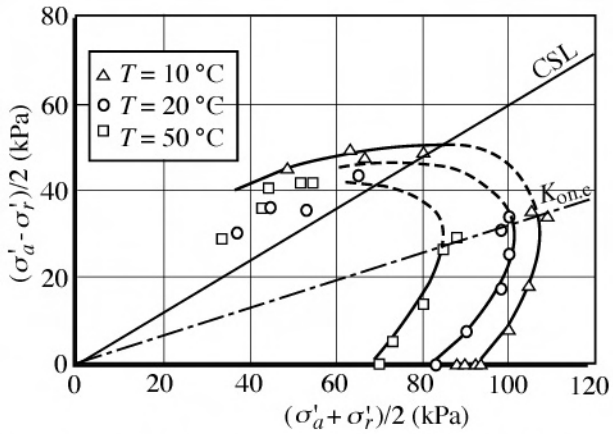

Figure 33. Limit state curves of Saint-Roch-de-l'Achigan clay (4.8 - 5.8 m) at temperatures of 10, 20 and 50 °C (after Marques *et al*., 2004)

heated to 50°C.

From behaviours previously described, the limit state surface in a e-p'-q diagram appears to have different peels, each one being associated with different strain rate and temperature (Fig. 34). The results also indicate that the mechanical behaviour could be normalized with respect to σ'_p, which is a function of strain rate and temperature. The isotache-isotherm model can thus be extended to 3-D conditions.

5.1.2 Shear and creep tests

Shear tests. Vaid & Campanella (1977) performed a variety of triaxial tests on the undisturbed Haney clay. In particular, they performed undrained compression tests at different strain rates, undrained compression tests in which the strain rate was changed at given strains, and creep tests. They concluded that the deviatoric stress, q, is a function of the shear strain, ε_s, and the rate of shear strain, $\dot{\varepsilon}_s$:

$$q = f(\varepsilon_s, \dot{\varepsilon}_s) \quad (19)$$

Tatsuoka et al. (2000, 2001) showed many other examples of shear tests performed on soft and stiff clays, silty sand, sand, mudstone and gravel that generally confirm Equation 19. It thus appears that the isotache model proposed by Šuklje (1957) for volumetric strains can be extended to shear strains and thus to the entire soil behaviour.

It is worth noting however that, at very small strains, the stress-strain behaviour may be perfectly elastic, thus not influenced by strain rate (see Tatsuoka et al. (2000) and Leroueil & Hight (2002)).

Creep tests. Many researchers, including Singh & Mitchell (1968), Bishop & Lovenbury (1969), Larsson (1977), Tavenas et al. (1978) and D'Elia (1991), observed that during long-term creep tests in triaxial conditions, the axial strain rate decreases with time and, for some cases closer to the failure envelope, after reaching a minimum value, the strain rate increases up to failure. Figure 35 shows typical creep test results obtained by Tavenas et al. (1978) on St-Alban clay.

Singh & Mitchell (1968) described the observed behaviour by the following equation:

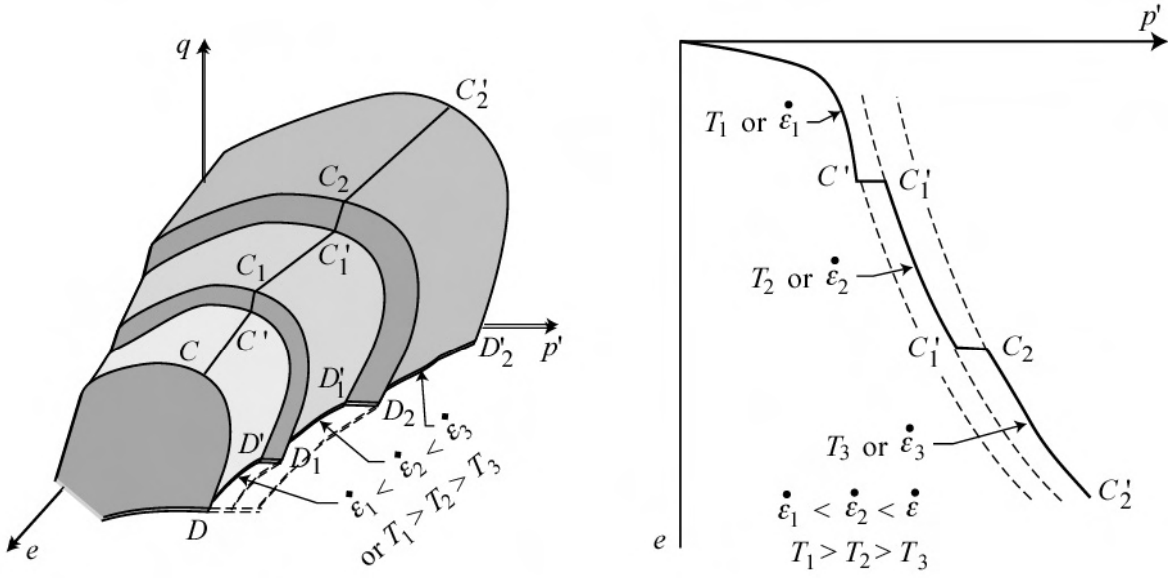

Figure 34. Influence of strain rate and temperature on the limit state surface of soils

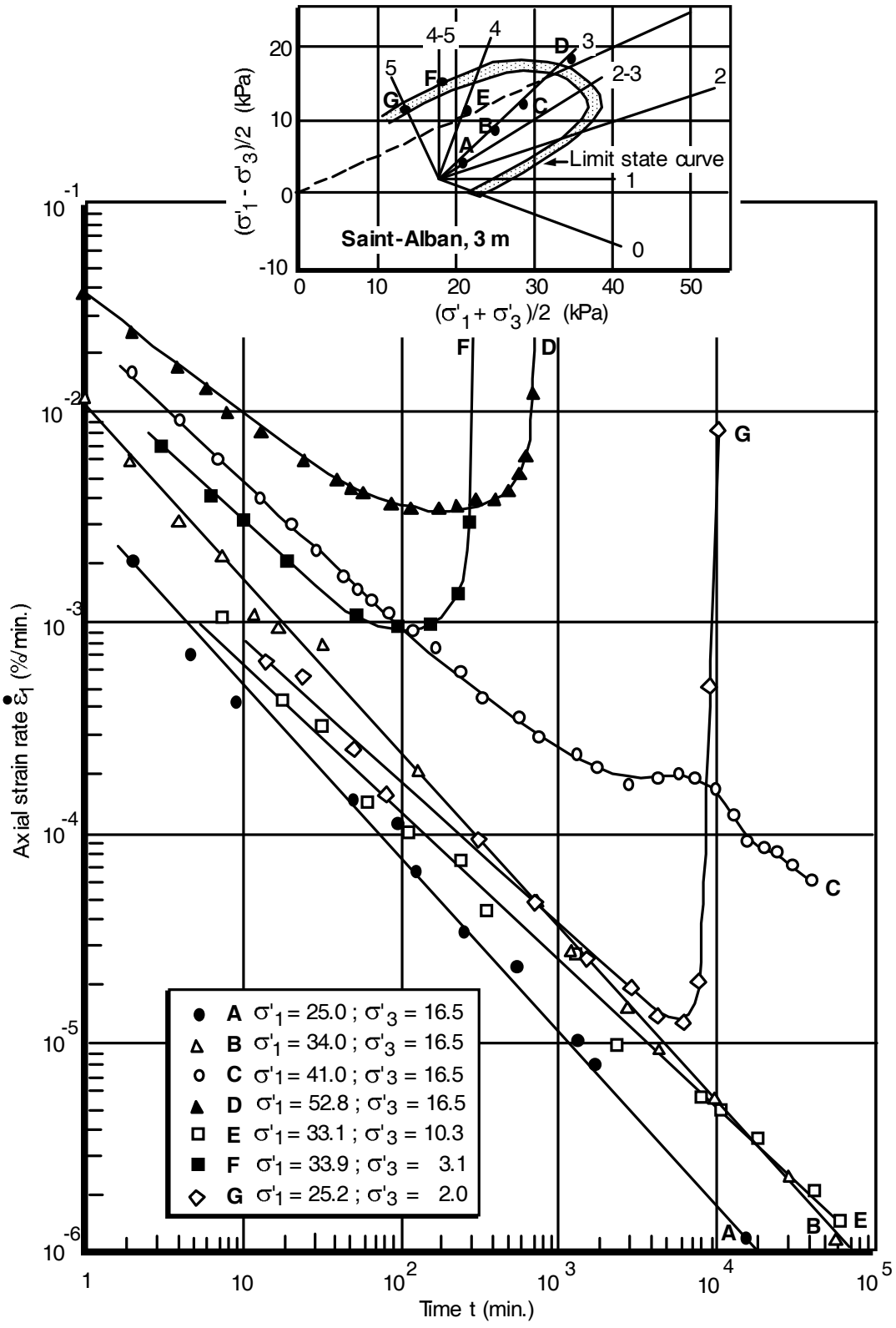

Figure 35. Axial strain rate-time relationship for creep tests on St-Alban clay (after Tavenas *et al.*, 1978)

$$\dot{\varepsilon}_1 = Ae^{\alpha q}\left(\frac{t_1}{t}\right)^m \qquad (20)$$

where $\dot{\varepsilon}_1$ is the axial strain rate at any time t, q is the stress level equal to the applied deviatoric stress divided by the deviatoric stress at failure in conventional compression tests, m is the slope of the log $\dot{\varepsilon}_1$-log t curve, t_1 is a reference time and α

and A are creep parameters. α is a different parameter than those used in Equations 9 and 17.

One difficulty with Equation 20 is that it does not satisfy the axiom of objectivity stated by Eringen (1975): "The constitutive response functionals must be form-invariant under arbitrary rigid motions of spatial frame and a constant shift of the origin of time." Indeed, in Equation 20, as well as in all equations in log t, a change in the origin of time modifies the form of the law and its parameters.

Marchand (1982) performed a series of triaxial tests on Mascouche clay: CIU, CAU and CAD tests at different strain rates; and long-term creep tests. Reanalysis of the results by Leroueil & Marques (1996) showed that conditions at failure for all these tests are strain rate dependent.

Wondering why creep behaviour as described by Equation 20 is time dependent whereas most aspects of soil behaviour are strain rate dependent, Leroueil (1998, 2001) examined this aspect on the basis of reasonable approximations and experience. The considered hypotheses were: a hyperbolic stress-strain curve; a log-log variation of shear strength with strain rate; and failure controlled by a critical accumulated strain, 0.9% in that case. The model, with the considered equations and parameters, is shown in Fig. 36a. Creep tests have been simulated for the deviatoric stresses indicated by arrows in Fig. 36a and the results are shown in Fig. 36b. It can be seen that the plots of logarithm of strain rate versus logarithm of time lines are essentially linear, as observed in laboratory tests (Fig. 35) and as indicated by Equation 20. As indicated by Leroueil (2001), this means that, fundamentally, soil behaviour is strain rate dependent and that the time model proposed by Singh & Mitchell (1968) reflects both this strain rate dependency and the test itself in which stress conditions for creep tests are suddenly applied at time zero.

5.2 Practical implications

The main practical implication of strain rate is that the strength mobilized during tests or in in situ conditions may be strain rate dependent.

Compiling test results obtained on 26 different clays, Khulawy & Mayne (1990) found a typical change in undrained shear strength of 10% per log cycle of strain rate (Fig. 37). Graham et al. (1983) found variations in triaxial compression, but also in triaxial extension and direct simple shear tests. It is interesting to note that the rate of variation with strain rate of the undrained shear strength, 10% per log cycle, is about the same as the rate of variation of the preconsolidation pressure with strain rate in inorganic clays (see Table 1). However, studies performed by Hight (1983), Hight et al. (1987) and Sheahan et al. (1996) on Lower Cromer till and Boston Blue clay indicate that the effect of strain rate on the compression undrained shear strength considerably decreases when the overconsolidation ratio increases.

Shear strength measured in situ follows the same tendency as shear strength in the laboratory. However, when the coefficient of consolidation of the soil in which the apparatus is inserted, the ge-

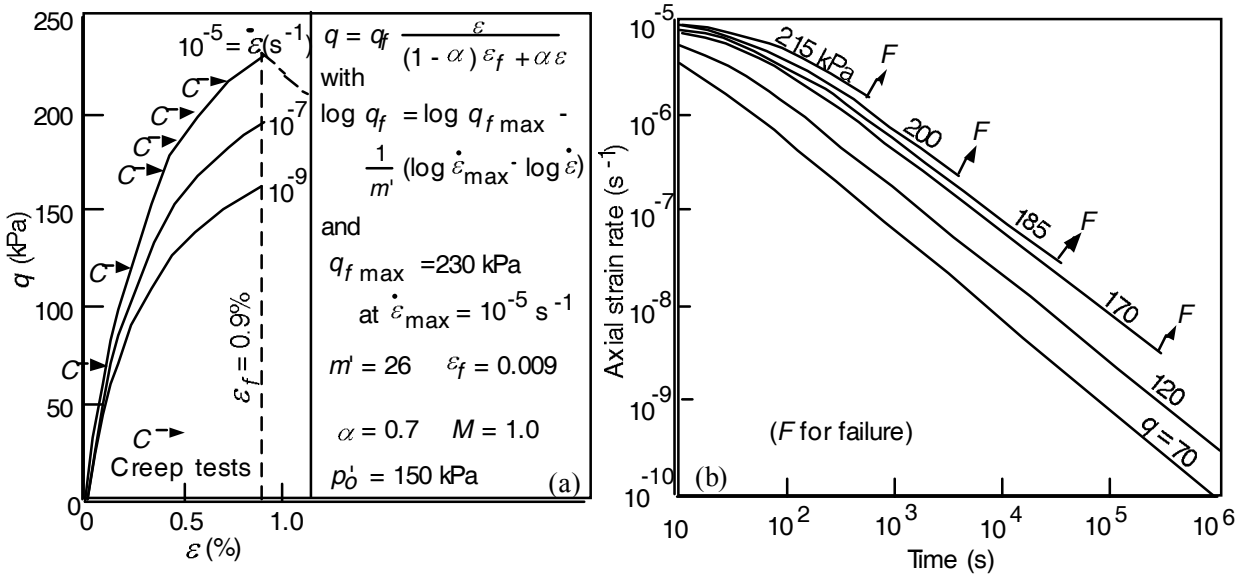

Figure 36. Simulation of creep tests: (a) strain rate dependency of the stress-strain behaviour and input parameters; (b) simulated creep tests for the conditions given in (a) (from Leroueil, 2001)

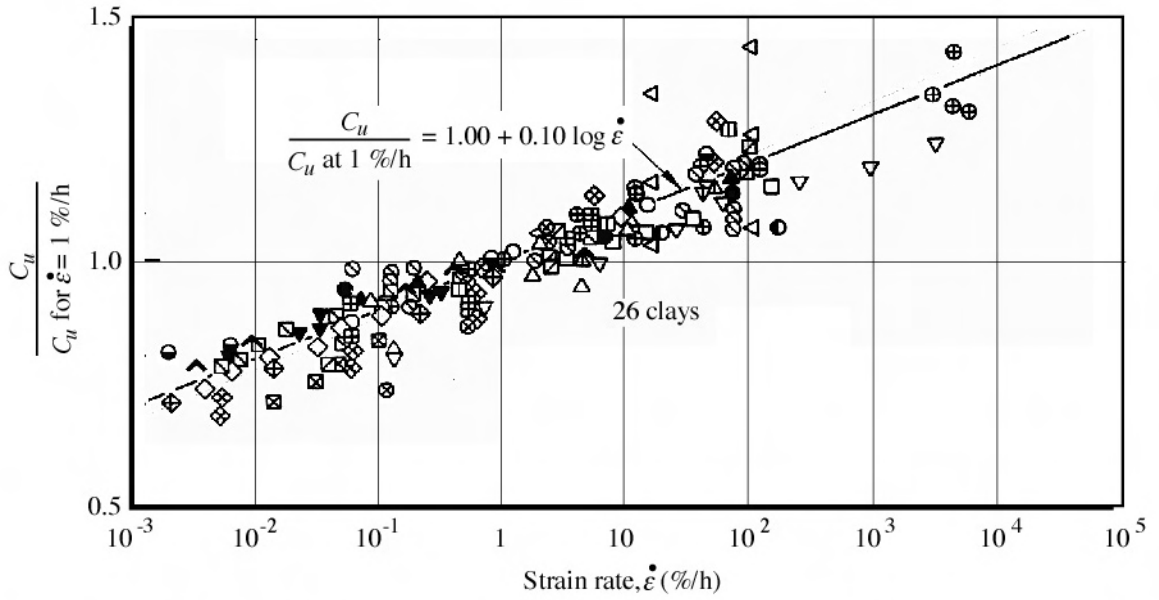

Figure 37. Influence of strain rate on the undrained shear strength measured in triaxial compression (from Kulhawy and Mayne, 1990)

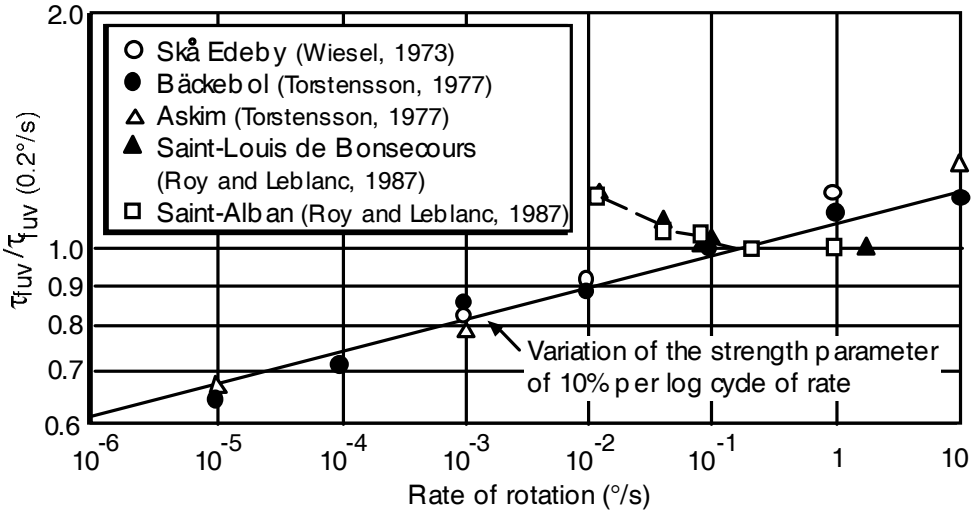

Figure 38. Influence of strain rate on vane shear strength (from Leroueil & Marques, 1996)

ometry of this apparatus and the rate of testing are such that partial consolidation occurs, the strength or "strength parameter" versus rate of testing relationship may diverge from the rheological curve.

Results from the literature are shown on Fig. 38 for the vane shear strength. It decreases by 10% per log cycle of the rate of rotation for Swedish clays. However, probably because of partial consolidation, the tests on St-Louis-de-Bonsecours and St-Alban clays show an increase in strength for rates of rotation lower than 0.1°/s. Similar rate effects can be observed for pressuremeter shear strength and penetrometer tip resistance (see Leroueil & Marques (1996) and Hight & Leroueil (2002) for details and references).

6 CONCLUSION

In 1957, Professor Suklje proposed the isotache model in which the compressibility of clays is strain rate dependent during both primary and secondary consolidation. Fifty years later, even if this concept is accepted by most of the researchers working in the domain, there are still a few who consider that it is not valid. Also, some aspects of the model have been specified or extended. The aim of the Paper is thus to try to summarize the information on the topic accumulated in the last 25 years or so.

The main conclusions deduced from laboratory testing are the following:

- Oedometer tests show that one-dimensional compression of clays is controlled by a unique effective stress-strain-strain rate model or, in other words by a set of isotaches. This set of isotaches can be described by two curves: one showing the variation of the preconsolidation pressure (or vertical effective stress at any void ratio) with strain rate; the second showing the normalized stress-strain curve. The first one is approximately linear when the logarithm of σ'_p is plotted as a function of the logarithm of strain rate, and the slope α is equal to $C_{\alpha e}/C_c$ and is thus constant for a given type of soils.
- Consolidation of a clay specimen divided in several sub-specimens show that the isotache set is continuous when the soil goes from primary consolidation to secondary consolidation.
- The isotache model should not be described in total strains but rather in terms of plastic strains. It may also have limitations associated with the fact that, in some soils and at low strain rates, microstructure may develop.

In in situ conditions, under an embankment, strain rates are generally much smaller than in laboratory tests. Consequently, according to the isotache model, the in situ compression curve should be below the compression curve obtained in the laboratory at the end-of-primary consolidation. This has two major implications: (a) at the end-of-primary consolidation, the strain in situ (or settlement) is larger than that calculated on the basis of laboratory tests; (b) at a given strain, the excess pore water pressure observed in situ is larger than the predicted one. A review of the literature shows that these implications are indeed observed for most of the well documented embankments. This review also indicates that α is probably not a constant, but decreases with strain rate.

An interesting case, for which contradictory conclusions were reached, is the Väsby test fill. It appears however that the discrepancy comes mostly from the quality of samples considered for comparing laboratory and in situ behaviours, the large compressibility obtained from low quality samples compensating for strain rate effect. Clearly identified in the case of Väsby, sampling disturbance could be a factor influencing the analysis of other cases.

In this author's opinion, there is no doubt that the isotache model applies to in situ conditions. Practical and simple methods for evaluating long-term settlements under embankments are proposed.

Laboratory tests have shown that soil compressibility is also influenced by temperature. They have also shown that the isotache model can be extended into an isotache-isotherm model. This model can be described by two functions, one giving the preconsolidation pressure, or the vertical effective stress at any void ratio, as a function of strain rate and temperature; the other being the normalized effective stress-strain curve. The form of the $\sigma'_p = f(\dot{\varepsilon}, T)$ relationship is the same for soils of a given type, indicating that it corresponds to a fundamental viscosity law.

It has also been shown that the entire limit state curve is controlled by strain rate and temperature; the shear strain-shear stress is also influenced by soil viscosity. The isotache-isotherm concept can thus be generalized to the entire soil behaviour. It obviously has several practical implications.

So, fifty years after its development by Professor Suklje, it is considered by this author that the isotache concept has been confirmed experimentally in the laboratory and in situ conditions, and that it can be extended to take into account the influence of temperature. The isotache-isotherm concept could also be extended to the general behaviour of soils.

REFERENCES

Aboshi, H. 1973. An experimental investigation on the similitude in the consolidation of a soft clay, including the secondary creep settlement. *Proc. 8th Int. Conf. on Soil Mech. and Found. Engng.,* Moscow, Vol. 4(3): 88.

Adachi, T., Oka, F. & Tange, Y. 1982. Finite element analysis of two dimensional consolidation using an elasto-viscoplastic constitutive equation. *Proc. 4th Int. Conf. on Numerical Methods in Geomechanics*, Edmonton, Vol. 1: 287-296.

Adachi, T., Oka, F. & Mimura, M. 1996. Modeling aspects associated with time dependent behavior of soils. *Session on Measuring and Modeling Time Dependent Soil Behavior*, ASCE Convention, Washington, Geot. Special Publication 61: 61-95.

Akai, K. 2000. Insiduous settlement of super-reclaimed offshore seabed. *Proc. Int. Symp. on Coastal Geotech. Engng. in Practice, Geo-Coast'91*, Yokohama, Vol. 1: 243-248.

Akai, K. & Tanaka, Y. 1999. Settlement behaviour of an offshore Airport KIA. *Proc. 12th European Conf. on Soil Mech. and Geotech. Engng.*, Amsterdam, Vol. 2: 1041-1046.

Arai, Y., Oikawa, K. & Yamagata, N. 1991. Large-scale sand drain works for the Kansai International Airport

Island. *Proc. Int. Symp. on Coastal Geotech. Engng. in Practice, Geo-Coast'91*, Yokohama, Vol. 1: 281-286.
Barden, L. 1965. Consolidation of clay with non-linear viscosity. *Géotechnique*, 15(4): 345-362.
Battelino, D. 1973. Oedometer testing of viscous soils. *Proc. 8th Int. Conf. on Soil Mech. and Found. Engng.*, Moscow, Vol. 1(1): 25-30.
Berre, T. & Iversen, K. 1972. Oedometer tests with different specimen heights on a clay exhibiting large secondary compression. *Géotechnique*, 22(1): 53-70.
Bishop, A.W. & Lovenbury, H.T. 1969. Creep characteristics of two undisturbed clays. *Proc. 7th Int. Conf. on Soil Mech. and Found. Engng*, Mexico City, 1: 29-37.
Bjerrum, L. 1967. Engineering geology of normally consolidated marine clays as related to the settlement of buildings. *Géotechnique*, 17(2): 83-119.
Boudali, M. 1995. *Comportement tridimensionnel et visqueux des argiles naturelles*. Ph.D. Thesis, Université Laval, Québec.
Boudali, M., Leroueil, S. & Murthy, B.R.S. 1994. Viscous behaviour of natural soft clays. *Proc. 13th Int. Conf. on Soil Mech. and Found. Engrg*., New Delhi, Vol. 1: 411-416.
Burghignoli, A. 1979. An experimental study of the structural viscosity of soft clays by means of continuous consolidation tests. *Proc. 7th European Conf. on Soil Mech. and Found. Engng.*, Brighton, Vol. 2: 23-28.
Burghignoli, A. & Desideri, A. 1988. Influenza della temperatura sulla compressibilità delle argille. *Gruppo Nazionale di Coodinamento per gli Studi di Ingegneria Geotecnica*, Convegno di Monselice: 193-206 (Ref. by Burghignoli et al. 1992).
Cao, L.F., Chang, M.-F., Teh, C.I. & Na, Y.M. 2001. Back-calculation of consolidation parameters from field measurements at a reclamation site. *Can. Geotech. J.*, 38(4): 755-769.
Casagrande, A. 1932. The structure of clay and its importance in foundation engineering. *Journal of the Boston Society of Civil Engineers:* 168-209.
Cekerevac, C. & Laloui, L. 200..
Chang, Y.C.E. 1981. *Long-term consolidation beneath the test fills at Väsby, Sweden*. Report No. 13, Swedish Geotechnical Institute, Linköping.
Crawford, C.B. 1965. The resistance of soil structure to consolidation. Can. Geotech. J., 2(2): 90-97.
Crooks, J.H.A., Becker, D.E., Jefferies, M.G. & McKenzie, K. 1984. Yield behaviour and consolidation – 1: pore pressure response. *Proc. ASCE Symp. on Sedimentation Consolidation Models: Predictions and Validation*, ASCE, pp. 356-381.
D'Elia, B. (1991). Deformation problems in the Italian structurally complex clay soils. *Proc. 10th European Conf. on Soil Mech. and Found. Engng.,* Florence, Vol. 4: 1159-1170.
Edil, T.B., Fox, P.J. & Lan, L.T. 1994. An assessment of one-dimensional peat compression. *Proc. 8th Int. Conf. on Soil Mech. and found. Eng.*, New Delhi, Vol. 1: 229-232.
Edil, T.B. & den Haan, E.J. 1994. Settlement of peats and organic soils. *Proc. Specialty Conf. on Vertical and Horizontal Deformations of Foundations and Embankments*, ASCE, Settlement '94, College Station, Vol. 2: 1543-1572.
Edil, T.B. & Fox, P.J. 1994. Field test of thermal precompression. *Proc. Specialty Conf. on Vertical and Horizontal Deformations of Foundations and Embankments*. ASCE, Settlement'94, College Station, Vol. 2: 1274-1286.
Eriksson, L.G. 1989. Temperature effects on consolidation properties of sulphide clays. *Proc. 12th Int. Conf. on Soil Mech. and Found. Engrg*., Rio de Janeiro,Vol. 3: 2087-2090.
Eringen, A.C. 1975. *Continuum Mechanics*, Vol. 2, Academic Press, New York.
Gibson, R.E. & Lo, K.Y. 1961. *A theory of consolidation for soils exhibiting secondary compression*. Report No. 41, Norwegian Geotechnical Institute, Oslo.
Graham, J., Crooks, J.H.A. & Bell, A.L. 1983. Time effects on the stress-strain behaviour of soft natural clays. *Géotechnique*, 33(3): 327-340.
Graham, J., Tanaka, N., Grilly, T. & Alfaro, M. 2001. Modified Cam-Clay modelling of temperature effects in clays. *Can. Geotech. J*., 38(3): 608-621.
Hansen, B. 1969. A mathematical model for creep phenomena in clay. *Proc. 7th Int. Conf. on Soil Mech. and Found. Engng.*, Mexico City, Specialty Session 12, pp. 12-18.
Hanzawa, H. 1989. Evaluation of design parameters for soft clays as related to geological stress history. *Soils & Foundations*, 29(2): 99-111.
Hawley, J.G. & Borin, D.L. 1973. A unified theory for the consolidation of clays. *Proc. 8th Int. Conf. on Soil Mech. and Found. Engng.*, Moscow, Vol. 1(3): 107-119.
Hight, D.W. 1983. *Laboratory investigation of sea bed clays*. Ph.D. Thesis, University of London.
Hight, D.W. , jardine, R.J. & Gens, A. 1987. The behaviour of soft clays. Chapter 2 of Embankments on Soft Clays, *Bulletin of the Public Works Research Center of Greece*, Athens: 33-38.
Hight, D.W. & Leroueil, S. 2002. Characterisation of soils for engineering purposes. *Proc. Int. Workshop on Characterisation and Engineering Properties of Natural Soils*, Singapore, Vol. 1: 255-352.
Houston, S.L., Houston, W.N. & Williams, N.D. 1985. Thermo-mechanical behavior of seafloor sediments. *J. Geotech. Engng. Div*., ASCE, 111(11): 1249-1263.
Hueckel, T. & Peano, A. 1987. Some geotechnical aspects of radioactive waste isolation in continental clays. *Computers and Geotech*., 3(2,3): 157-182.
Hueckel, T. & Baldi, G. 1990. Thermoplasticity of saturated clays: Experimental constitutive study. *J. Geotech. Engng. Div.*, ASCE, 116(12): 1778-1796.
Imai, G. 1995. Analytical examinations of the foundations to formulate consolidation phenomena with inherent time-dependence. *Proc. Int. Symp. on Compression and Consolidation of Clayey Soils - IS-Hiroshima's 95*, Hiroshima, 2: 891-935.
Imai, G. & Tang, Y. 1992. A constitutive equation of one-dimensional consolidation derived from interconnected tests. *Soils & Foundations*, 32(2): 83-96.
Imai, G., Ohomukai, N. & Tanaka, H. 2005. An isotaches-type model for predicting long-term consolidation of KIA clays. *Proc. Symp. on Geotechnical Aspects of Kansai international Airport*, Kansai Airport, pp. 49-64.

Jamiolkowski, M., Ladd, C.C., Germaine, J.T. & Lancellotta, R. 1985. New developments in field and laboratory testing of soils. *Proc.11th Int. Conf. on Soil Mech. and Found. Engrg.*, San Francisco, Vol. 1, pp. 57-153.

Kabbaj, M. 1985. *Aspects rhéologiques des argiles naturelles en consolidation*. Ph.D. Thesis, Université Laval, Québec.

Kabbaj, M., Oka, F., Leroueil, S. & Tavenas, F. 1986. Consolidation of natural clays and laboratory testing. *Proc. Conf. on Consolidation of Soils: Testing and Evaluation*. American Society for Testing and Materials, Special Technical Publication STP 892, pp. 378-404.

Kabbaj, M., Tavenas, F. & Leroueil, S. 1988. In situ and laboratory stress-strain relations. *Géotechnique*, 38(1): 83-100.

Kim, Y.T. & Leroueil, S. 2001. Modelling the viscoplastic behaviour of clays during consolidation : application to Berthierville clay in both laboratory and field conditions. Can. Geotech. J., 38(3): 484-497.

Kobayashi, M., Furudoi, T., Suzuki, S. & Watabe, Y. 2005. Modeling of consolidation characteristics of clays for settlement prediction of Kansai International Airport. *Proc. Symp. on Geotechnical Aspects of Kansai International Airport*, Kansai Airport, pp. 65-76.

Koppejan, A.W. 1948. A formula combining the Terzaghi load compression relationship and the Buisman secular time effect. *Proc. 2nd Int. Conf. on Soil Mech. and Found. Engng.*, Rotterdam, Vol. 3: 32-37.

Kulhawy, F.H. & Mayne, P.W. 1990. *Manual of estimating soil properties for foundation design*. Geotechnical Engineering Group, Cornell University, Ithaca.

Ladd, C.C., Foott, R., Ishihara, K., Schlosser, F. & Poulos, H.G. 1977. Stress-deformation and strength characteristics. State-of–the-Art Report, *Proc. 9th Int. Conf. on Soil Mech. & Found. Engrg.*, Tokyo, Vol. 2, pp. 421-494.

Laloui, L. & Cekerevac, C. 2003. Thermo-plasticity of clays: An isotropic yield mechanism. *Computers and Geotechnics*, 30: 649-660.

La Rochelle, P., Sarrailh, J., Tavenas, F., Roy, M. & Leroueil, S. 1981. Causes of sampling disturbance and design of a new sampler for sensitive soils. *Can. Geotech. J.*, 18(1): 52-66.

Larsson, R. 1977. *Basic behaviour of Scandinavian soft clays.* Report No. 4, Swedish Geotechnical Institute, Linköping.

Larsson, R. 1981. *Drained behaviour of Swedish clays*. Report No. 12, Swedish Geotechnical Institute, Linköping.

Larsson, R. 1986. *Consolidation of soft soils*. Report No. 29, Swedish Geotechnical institute, Linköping.

Larsson, R. & Mattsson, H. 2003. *Settlements and shear strength increase below embankments*. Report 63, Swedish Geotechnical Institute, Linköping.

Leonards, G.A. 1977. *Proc. 9th Int. Conf. on Soil Mech. and Found. Engng.*, Tokyo, Panel discussion, Vol. 3: 384-386.

Leonards, G.A. & Altschaeffl, A.G. 1964. Compressibility of clay. *J. of the Soil Mech. and Found. Engrg. Div., ASCE*, 90(5): 133-155.

Leroueil, S. 1988. Tenth Canadian Geotechnical Colloquium: Recent developments in consolidation of natural clays. *Can. Geotech. J.*, 25(1): 85-107.

Leroueil, S. 1996. Compressibility of clays: fundamental and practical aspects. *J. Geotech. Engrg. Div.*, ASCE, 122(7): 534-543. Also partially published in the *Proc. of the ASCE Conf. on Vertical and Horizontal Deformations of Foundations and Embankments*, Settlement's 94, College Station, Vol. 1: 57-76.

Leroueil, S. 1998. Elements of time-dependent mechanical behaviour of overconsolidated clays. *Proc. 51st Can. Geotech. Conf.*, Edmonton, Vol. 2: 671-677.

Leroueil, S. 2001. Natural slopes and cuts: movement and failure mechanisms. *Géotechnique*, 51(3): 197-243.

Leroueil, S. & Kabbaj, M. 1987. Discussion on Settlement analysis of embankments on soft clays. *J. Geotech. Engng. Div.*, ASCE, 113(9) : 1067-1070.

Leroueil, S. & Hight, D.W. 2002. Behaviour and properties of natural soils and rocks. *Proc. Workshop on Characterisation and Properties of Natural Soils*, Singapore, Vol. 1: 29-254.

Leroueil, S., Samson, L. & Bozozuk, M. 1983a. Laboratory and field determination of preconsolidation pressure at Gloucester. *Can. Geotech. J.*, 20(3): 477-490.

Leroueil, S., Tavenas, F., Samson, L. & Morin, P. 1983b. Preconsolidation pressure of Champlain clays - Part II: Laboratory determination. *Can. Geotech. J.*, 20(4): 803-816.

Leroueil, S., Kabbaj, M., Tavenas, F. & Bouchard, R. 1985a. Stress-strain-strain rate relation for the compressibility of sensitive natural clays. *Géotechnique*, 35(2): 159-180.

Leroueil, S., Kabbaj, M. & Tavenas, F. 1985b. Discussion on Theme Lecture No. 2-B on Laboratory Testing. *Proc. 11th Int. Conf. on Soil Mech. and found. Engng.*, San Francisco, Vol. 5 : 2691-2692.

Leroueil, S., Kabbaj, M., Tavenas, F. & Bouchard, R. 1986. Closure to "Stress-strain-strain rate relation for the compressibility of sensitive natural clays". *Géotechnique*, 36(2): 288-290.

Leroueil, S., Kabbaj, M. & Tavenas, F. 1988. Study of the validity of a $\sigma'_v - \varepsilon_v - \dot{\varepsilon}_v$ model in in situ conditions. *Soils & Foundations,* 28(3): 3-25.

Leroueil, S. & Vaughan, P.R. 1990. The general and congruent effects of structure in natural soils and weak rocks. *Géotechnique,* 40(3): 467-488.

Leroueil, S. & Marques, M.E.S. 1996. Importance of strain rate and temperature effects in geotechnical engineering. *Session on Measuring and Modeling Time Dependent Soil Behavior*, ASCE Convention, Washington, Geot. Special Publication 61: 1-60.

Leroueil, S., Perret, D. & Locat, J. 1996. Strain rate and structuring effects on the compressibility of a young clay. *Session on Measuring and Modeling Time Dependent Soil Behavior*, ASCE Convention, Washington, Geot. Special Publication 61: 137-150.

Lingnau, B.E., Graham, J., & Tanaka, N. 1995. Isothermal modeling of sand-bentonite mixtures at elevated temperatures. *Can. Geotech. J.*, 31(1): 78-88.

Lo, K.Y. & Morin, J.P. 1972. Strength anisotropy and time effects of two sensitive clays. *Can. Geotech. J.*, 9(3): 261-277.

Magnan, J.-P. 1992. Le rôle du fluage dans les calculs de consolidation et de tassement des sols compressibles. *Bulletin de Liaison des Laboratoires des Ponts et Chaussées, 180 : 18-24.*

Marchand, G. 1982. *Quelques considérations sur le comportement avant rupture des pentes argileuses naturelles*. M.Sc. Thesis, Université Laval, Québec, Canada.

Marques, M.E.S. & Leroueil, S. 2005. *Preconsolidating clay deposit by vacuum and heating in cold environment*. Chapter, Book on Ground Improvement Case Histories, Elsevier, U.K.

Marques, M.E.S., Leroueil, S. & Almeida, M. de S.S. (2004). Viscous behaviour of St-Roch-de-l'Achigan clay, Québec. *Can. Geotech. J.*, 41(1): 25-38.

Mesri, G. 1987. The fourth law of soil mechanics: the law of compressibility. *Proc. Int. Symp. on Geotech. Engng. of Soft Soils*, Mexico City, Vol. 2: 179-187.

Mesri, G., & Godlewski, P.M. 1977. Time and stress compressibility interrelationships. *J. Geotech. Enging Div., ASCE*, 103(GT5): 417-430.

Mesri, G. & Choi, Y.K. 1985a. Settlement analysis of embankments on soft clays. *J. Geotech. Engng., ASCE,* 111(4): 441-464.

Mesri, g. & Choi, Y.K. 1985b. The uniqueness of the end -of-primary (EOP) void ratio-effective stress relationship. *Proc. 11th ICSMFE, San Francisco,* Vol. 2: 587-590.

Mesri, G. & Feng, T.W. 1986. Discussion of "Stress-strain-strain rate relation for the compressibility of sensitive natural clays" by S. Leroueil, M. Kabbaj, F. Tavenas & R. Bouchard. *Géotechnique*, 36(2): 283-287.

Mesri, G., Lo, D.O.K. & Feng, T.W. 1994. Settlement of embankments on soft clays. *Proc. Specialty Conf. on Vertical and Horizontal Deformations of Foundations and Embankments*, *ASCE*, Settlement'94, College Station, Vol. 1: 8-56.

Mesri, G., Shahien, M. & Feng, T.W. 1995. Compressibility parameters during primary consolidation. *Proc. Int. Symp. on Compression and Consolidation of Clayey Soils - IS-Hiroshima's 95*, Hiroshima, Vol. 2: 1021-1037.

Miliziano, S. 1992. *Effetti della temperature sul comportamento meccanico delle terre coesive*. Ph.D thesis, Università di Roma "La Sapienza", Rome. Italy.

Mimura, M. & Jang, W.J. 2005. Long-term settlement of the Pleistocene deposits due to construction of KIA. *Proc. Symp. on Geotechnical Aspects of Kansai international Airport*, Kansai Airport, pp. 77-86.

Mitchell, J.K. 1964. Shearing resistance of soils as a rate process. *J. Soil Mech. and Found Engng. Div.*, ASCE, 90(1):29-61.

Mitchell, J.K. 1993. *Fundamentals of soil behavior.* 2nd Ed., John Wiley & Sons, Inc.

Mitchell, J.K. & Solymar, Z.V. 1984. Time-dependent strength gain in freshly deposited or densified sand. *J. of Geotech. Engrg.*, *ASCE*, 110(11): 1559-1576.

Morin, P., Leroueil, S. & Samson, L. 1983. Preconsolidation pressure of Champlain clays. Part I: In situ determination. *Can. Geotech. J.,* 20(4): 782-802.

Moritz, L. 1995a. *Geotechnical properties of clay at elevated temperatures*. Report No. 47, Swedish Geotechnical Institute, Linköping.

Moritz, L. 1995b. Geotechnical properties of clay at elevated temperatures. *Proc. Int. Symp.on Compression and Consolidation of Clayey Soils – IS-Hiroshima's 95*, Hiroshima, Vol. 1: 267-272.

Murayama, S. & Shibata, T. 1961. Rheological properties of clays. *Proc. 5th Int. Conf. on Soil Mech. and Found. Engng.*, Paris: 269-273.

Rowe, R.K. & Hinchberger, S.D. 1998. The significance of rate effects in modeling the Sackeville test embankment. Can. Geotech. J., 35: 500-516.

Sällfors, G. 1975. *Preconsolidation pressure of soft high plastic clays*. Ph.D. Thesis, Chalmers University of Technology, Gothenburg, Sweden.

Schmertmann, J.H. 1991. The mechanical aging of soils. *J. of Geotech. Engng.*, ASCE, 117(9): 1288-1330.

Sheahan, T.C., Ladd, C.C. & Germaine, J.T. 1996. Rate dependent undrained behaviour of saturated clay. *J. Geotech. Engng.*, ASCE, 122(2): 99-108.

Singh, A.W. & Mitchell, J.K. 1968. General stress-strain-time function for soils. *J. Soil Mech. and Found. Engng. Div*., *ASCE*, 94(1): 21-46.

St-Arnaud, G., Morel, R. & Lavallée, J.-G. 1992. Comportement de la foundation argileuse traitée avec des drains synthétiques sous le remblai d'essai Olga-C. *Internal Report,* Hydro-Québec, Montréal, Québec.

Šuklje, L. 1957. The analysis of the consolidation process by the isotache method. *Proc. 4th Int. Conf. on Soil Mech. and Found. Engng*., London, Vol.1, pp. 200-206.

Šuklje, L. 1969a. *Rheological aspects of soil mechanics*. Wiley, London.

Šuklje, L. 1969b. Consolidation of viscous soils subjected to continuously increasing uniform load. In *New Advances in Soil Mechanics*, Vol. 1: 199-235, Praha.

Šuklje, L. 1982. On some controversial effects of the viscous structural resistance of soils. *Acta Geotech*. No. 84.

Šuklje, L. & Majes, B. 1988. Consolidation and creep of soils in plane-strain conditions. *Géotechnique*, 39(2): 231-250.

Švano, G., Christensen, S. & Nordal, S. 1991. A soil model for consolidation and creep. *Proc. 10th European Conf. on Soil Mech. and found. Engng.*, Florence, Vol. 1: 269-272.

Szavits-Nossan, V. 1988. *Intrinsisc time behavior of cohesive soils during consolidation*. Ph.D. Thesis, Univ. of Colorado, Boulder.

Tatsuoka, F., Santucci de Magistris, F., Hayano, K., Momoya, Y. & Koseki, J. 2000. Some new aspects of time effects on the stress-strain behaviour of stiff geomaterials. *Proc. 2nd Int. Symp. on the Geotechnics of Hard Soils – Soft Rocks*, Naples, Vol. 3 : 1285-1371.

Tatsuoka, F., Uchimura, T., Hayano, K., Di Benedetto, H. Koseki, J. & Siddiquee, M.S.A. 2001. Time dependent deformation characteristics of stiff geomaterials in engineering practice. *Proc. 2nd Int. Conf. on Pre-Failure Deformation Characteristics of Geomaterials,* Torino, Vol. 2: 1161-1250.

Tavenas, F., Leroueil, S., La Rochelle, P. & Roy, M. 1978. Creep behaviour of an undisturbed lightly overconsolidated clay. *Can. Geotech. J*., 15(3): 402-423.

Taylor, D.W. 1942. *Research on consolidation of clays*. Series 82, Massachusetts Inst. of Technol., Cambridge, Mass.

Taylor, D.W. & Merchant, W. 1940. A theory of clay consolidation accounting for secondary compression. *J. Math. Phys.,* 19: 167-185.

Tidfors, M. & Sällfors, G. 1989. Temperature effect on the preconsolidation pressure. *Geotechnical Testing J.,* 12(1): 93-97.

Vaid, Y.P. & Campanella, R.G. 1977. Time-dependent behaviour of undisturbed clay. *J. Geotech. Engrg. Div.*, *ASCE*, 103(7): 693-709.

Vaughan, P.R. 1994. 34th Rankine Lecture: Assumption, prediction and reality in geotechnical engineering. *Géotechnique*, 44(4): 571-609.

Yashima, A., Leroueil, S. & Oka, F. 1997. Modelling temperature and strain rate dependent behavior of clays : one-dimensional consolidation. *Soils & Foundations*, 38(2): 63-73.

Yin, J.H., Graham, J., Clark, J.L. & Gao, L. 1994. Modelling unanticipated pore-water pressures in soft clays. *Can. Geotech. J.*, 31: 773-778.

Yoshikuni, H., Nishiumi, H., Ikegami, S. & Seto, K. 1994. The creep and effective stress-relaxation behavior on one-dimensional consolidation (in Japanese). *Proc. 29 th Japan National Conf. on Soil Mech. and Found. Engrg.*, 29: 269-270.

Yoshikuni, H., Kusakabe, O., Okada, M., & Tajima, S. 1995. Mechanism of one-dimensional consolidation. *Proc. Int. Symp. on Compression and Consolidation of Clayey Soils - IS-Hiroshima's 95*, Hiroshima, 1(4): 97-504.